# Fabrication of
# Zinc Oxide Thin Films
# For Renewable Energy and Sensor Applications

A thesis submitted in partial fulfillment

Of the requirements for the degree of

Master of Science

In Engineering

By

**Theresa Yvonne Hill**

B.S.Ch.E.

University of Cincinnati, 1982

2010

Wright State University

WRIGHT STATE UNIVERSITY

SCHOOL OF GRADUATE STUDIES

November 10,2010

I HEREBY RECOMMEND THAT THE THESIS PREPARED UNDER MY SUPERVISION BY Theresa Yvonne Hill ENTITLED Fabrication of Zinc Oxide Thin Films For Renewable Energy and Sensor Applications BE ACCEPTED IN PARTIAL FULFILLMENT OF THE REQUIREMENTS FOR THE DEGREE OF Master of Science in Engineering.

Dr. Hong Huang, Ph.D.
Thesis Director

George Huang, Ph.D.
Chair Department of
Mechanical and Material
Engineering
College of Engineering and
Computer Science

Committee on
Final Examination

Ioana Pavel, Ph.D.

Sharmila Mukhopadhyay,Ph.D.

Andrew Hsu, Ph.D.
Dean, School of Graduate Studies

## Abstract

Hill, Theresa Yvonne. M. S. Eng., Department of Mechanical and Materials Engineering, Wright State University, 2010. Fabrication of Zinc Oxide Thin Films for Renewable Energy and Sensor Applications.

Progress in commercializing renewable energy technologies is being advanced by developments in Zinc Oxide material science. The photovoltaic cell, for example, generates electricity by receiving solar energy into the cell, generating electrons, and simultaneously transporting electrical charge out of the cell. Metals are capable of removing electrical charge but block transmission of sunshine. Glass and plastics are capable of transmitting sunshine but block the removal of electrical charge. Therefore an exterior layer that is both optically transparent and electrically conductive is desirable. Transparent conductive oxides (TCOs) are the ideal material for such applications since they are capable of both functions. In addition, the unique opto-electronic properties of TCOs make them suitable for many other applications such as dye sensitized solar cells and sensor devices.

Zinc oxide is a non-toxic and inexpensive TCO material in comparison with the state-of-the-art tin-doped indium oxide (ITO). Therefore, optimizing the fabrication of high-quality zinc oxide thin films at low cost plays a significant role in the advancement of solar technology commercialization. The sol-gel process has advantages over other techniques in terms of low-cost, feasible mass production. In this work, key variables affecting zinc oxide sol-gel processing were investigated. Resulting films were characterized for optical transparency by UV-VIS spectrophotometry. Chemical reaction mechanisms within the sol-gel process and Zinc Oxide film crystalline properties were analyzed using Raman spectroscopy. Key variables affecting final film quality were explored.

# Contents

Chapter 1: Zinc Oxide Thin Films for Renewable Energy and Sensor Applications ..... 1

Section I: Review of Zinc Oxide Properties ..... 1

Part a: ZnO Crystal Structures ..... 1

Part b: ZnO Electronic Properties for Renewable Energy Applications ..... 4

Part c: ZnO Optical Properties for Renewable Energy Applications ..... 5

Part d: Other ZnO Properties for Sensor Applications ..... 5

Section II: Applications and Opportunities for Zinc Oxide Thin Films in Renewable Energy Technology ..... 7

Part a: Applications and Opportunities for Zinc Oxide Thin Films in Solar Cells ..... 7

Part b: Applications and Opportunities for Zinc Oxide in Dye Sensitized Solar Cells ..... 11

Part c: Other Applications and Opportunities for Zinc Oxide Thin Films as Sensors ..... 13

Section III: Scope of Zinc Oxide Thin Film Sol-Gel Research ..... 15

Chapter 2: Technology for Zinc Oxide Thin Film Fabrication ..... 17

Section I: Overview of Thin Film Technology ..... 17

Section II: Zinc Oxide Thin Film Technology ..... 20

Section III: Zinc Oxide Sol-Gel Thin Film Technology ..... 21

Chapter 3: Fabrication of ZnO Thin Films Using Organic Based Sol-Gel ..... 33

Section I: Identification of Key Factors Controlling Organic Based ZnO Sol-Gel ..... 33

Section II: Evaluation of Key Factors Controlling Organic Based ZnO Sol-Gel ..... 35

Section III: Series to Duplicate and Expand Organic Based ZnO Sol-Gel Series ..... 39

Section IV: Film Synthesis via Spontaneous 'Self Assembly' in Organic ZnO Sol-Gel ..... 42

Chapter 4: Fabrication of ZnO Thin Films Using Aqueous Sol-Gel ..... 45

Section I: Identification of Key Variables Controlling Aqueous ZnO Sol-Gel Synthesis.....45

Part a: Aqueous ZnO Sol-Gels with pH modifier Citric Acid .....45
Part b: Influence of Ammonium Hydroxide on Aqueous ZnO Sol-Gel .....46
Part c: Influence of Monoethanolamine on Aqueous Zinc Oxide Sol-Gels .....48
Part d: Influence of Ammonium Hydroxide plus Citric Acid on Aqueous ZnO Sol-Gels.....48

Section II: Evaluation of Key Variables in Film Formation of Aqueous ZnO Sol-Gels.....51

Part a: Initial evaluation of Key Variables in Film Formation of Aqueous ZnO Sol-Gels .....51
Part b: Modification of Aqueous ZnO Sol-Gel Formulation to Achieve Film Formation.....52
Part c: Final Evaluation of Aqueous ZnO Sol-Gel Film Formation .....53

Chapter 5: Optical Performance of ZnO Thin Film via UV-Vis Spectrophotometry .....55

Section I: Background on UV-Vis Spectrophotometry .....55
Section II: Optical Properties of ZnO Films vs. Low Temperature Thermal Treatments.....57
Section III: Optical Properties of ZnO Films vs. High Temperature Thermal Treatments .....59
Section IV: Optical Properties of ZnO Thins Films vs. Organic Solvent .....63
Section V: Optical Properties vs. ZnO Aqueous Sol-Gel .....65

Chapter 6: Mechanistic Understanding via Raman Spectroscopy .....68

Section I: Raman Spectroscopy Methodology .....68
Section III: Mechanistic Understanding of Sol Chemistry .....73
Section IV: ZnO Films by Self- Assembly.....80
Section V: ZnO Thin Films Thermal.....85

Chapter 7: Conclusions and Future Work .....88
Bibliography.....96

# List of Figures

Figure 1: Zinc Oxide Crystal Structures ..... 3
Figure 2: Anatomy of a PV Solar Cell ..... 8
Figure 3: Antireflective Layer ..... 10
Figure 4: Diagram of a DSSC ..... 11
Figure 5: Sol-Gel Process ..... 18
Figure 6: SEM images of ZnO Fabricated by Molecular Beam Epitaxy ..... 20
Figure 7: SEM micrographs of ZnO films prepared by Sol-Gel ..... 21
Figure 8: Zinc Acetate Sol-Gel Chemistry ..... 23
Figure 9: Thin Film Formation Steps ..... 29
Figure 10: Process Flow Chart for ZnO Sol-Gel Films ..... 35
Figure 11: Pictures of Organic Based Sol vs. Water as a Solvent ..... 37
Figure 12: Photos of Zinc Oxide Films for 0.5 M Zinc Acetate Sols ..... 37
Figure 13: Photos of Zinc Oxide Films for 1.3 M Zinc Acetate Sols ..... 38
Figure 14: pH Modifier Comparison ..... 39
Figure 15: Film from Water Based ZnO Sol ..... 39
Figure 16: UV-VIS Spectrophotometry ..... 55
Figure 17: Low Drying Temperatures vs. Optical Properties ..... 58
Figure 18: Annealing Temperature vs. Optical Properties ..... 61
Figure 19: Band Gap Absorption Profile vs. Thermal Treatment ..... 62
Figure 20: Observed Blue Shift at Low Thermal Treatments ..... 63
Figure 21: Optical Properties of ZnO Thin Films from Different Organic Solvents ..... 65
Figure 22: Optical Properties vs. Aqueous Sol-Gel with PVA ..... 66
Figure 23: Atomic Force Microscopy of Aqueous Sol-Gel Film with PVA ..... 66
Figure 24: Raman Spectroscopy by Adam Stahler ..... 69
Figure 25: Raman spectra from Reference 42 of ZnO Thin Films ..... 71
Figure 26: Raman Spectra of MOE Sol-Gel Fabricated Six Weeks Apart. ..... 73

Figure 27: Raman Spectra of MOE sol and Precursor Materials. ..... 75
Figure 28: Raman Spectra of Butanol Sol and Precursor Materials. ..... 76
Figure 29: Raman spectra of IPA sol vs. Precursors & ZnO 'self-assembly' Film ..... 77
Figure 30: Methanol Sol-Gel Raman of Solution and Gel Phase ..... 79
Figure 31: Raman Spectra of ZnO 'Self-Assembly' Film vs. ZnO Bulk ..... 81
Figure 32: Zinc Oxide Thin Film formed by Methanol Sol-Gel 'Self-Assembly' ..... 84
Figure 33 Raman Spectra of ZnO Thin Films with Thermal Annealing ..... 86
Figure 34: Surfactant Phases ..... 92
Figure 35: Proposed Model for Organic Solvent Bridging Mechanism ..... 93

# List of Tables

Table 1: Physical Properties of ZnO ..... 2
Table 2: Zinc Oxide Sol-Gel Literature Reports on Zinc Acetate Concentration ..... 24
Table 3: Zinc Oxide Sol-Gel Literature Report on pH Modifier Level ..... 25
Table 4: Zinc Oxide Sol-Gel Literature Reports on Film Substrate ..... 28
Table 5: Zinc Oxide Sol-Gel Literature Reports on Initial Drying Temperatures ..... 30
Table 6: Zinc Oxide Sol-Gel Literature Reports on Annealing Temperatures ..... 31
Table 7: Influence of Citric Acid on Aqueous Zinc Acetate Solutions ..... 46
Table 8: Influence of Ammonium Hydroxide on Aqueous Zinc Acetate Solutions ..... 47
Table 9: Influence of Monoethanolamine on Aqueous Zinc Acetate Solutions ..... 48
Table 10: Influence of $NH_3OH$ plus Citric Acid on Aqueous ZnO Sol-Gel ..... 49
Table 11: Polymeric Thickening Agents ..... 54
Table 12: Solvent Boiling Point Data ..... 65
Table 13: Material Properties ..... 95

# List of Equations

Equation 1: ZnO Defect Chemistry……..Page 15

Equation 2: ZnO Defect Chemistry……..Page 15

Equation 3: ZnO n-type Doping……Page 15

Equation 4: ZnO p-type Doping……Page 16

Equation 5: ZnO p-type Doping……Page 16

Equation 6: Condensation Reaction forming Zinc Oxide……Page 38

Equation 7: Band Gap Calculations……Page 55

Equation 8: Band Gap Calculations for Zinc Oxide……Page 56

Equation 9: Absorption Equation for Cary UV-Vis Spectrophotometry…….Page 56

Equation 10: %Transmission from UV-Vis Absorption Data ……Page 56

## Acknowledgments

I would like to express my heartfelt thanks to the many people who have guided me through this research project. Their supervision, direction, and support have been invaluable to me. I would like to begin by giving special thanks go to my advisor, Dr. Hong Huang. I feel extremely fortunate to have been blessed with such a wonderful advisor. Dr. Huang provided countless hours to advise, guide, support and offer key insights that were essential to moving my research forward.

I also want to extend heartfelt thanks to Dr. Ioana Pavel and her wonderful team of graduate students in the Wright State University Chemistry Department. I will be forever grateful to Dr. Pavel for generously providing the technical support and the expert analyses needed to obtain and make sense of the UV-Vis and Raman spectroscopy data. I also want to thank Dr. Pavel for her participation in the review panel for this thesis research.

Special thanks to several people in Dr. Pavel's group of graduate students. First of all, a huge 'thank you' to Adam Stahler who provided numerous hours of his time to develop Raman methods and obtain the Raman spectra that have made this research cutting-edge. Special thanks also to Nora Hunter and Arathi Paluri for their help in training and supervising my work with the UV-Vis spectrophotometer that was so essential to the characterization of my films.

I also want to express my thanks to Dr. Sharmila Mukhopadhyay - first of all for her participation in the review panel for this thesis research. But I also want to express thanks to Dr. Mukhopadhyay for the three classes I took with her which gave me a solid foundation for doing this research project!

I will be forever grateful to Dr. George Huang, the chairman of the Mechanical and Materials Engineering Department, for making the opportunity to be a part of the new 'Renewable and Clean Energy Master's Program' a reality.

I also want to thank my class mates especially Joe Bozeman, Jared McCoppin, Hema Vijwani and Sree Lakshmi Cheekati who supported me with friendship and encouragement as I progressed through my thesis research.

Finally, I would like to thank my family, my dear husband and son, as well as my extended family. Their unfailing love and belief in my ability to succeed has been the ‘wind beneath my wings’.

## Dedication

I would like to dedicate this paper to the memory of my mother, Patricia Durchholz, who always encouraged the pursuit of higher education regardless of the challenge and barriers involved.

# Chapter 1: Zinc Oxide Thin Films for Renewable Energy and Sensor Applications

## Section I: Review of Zinc Oxide Properties

Zinc Oxide is an inorganic compound which usually appears as a white powder. Physical properties are detailed in Table 1. The chemical bonds that form Zinc Oxide are borderline between ionic and covalent bonds though they lean towards being ionic. ZnO has relatively low solubility in water ($1.6 \times 10^{-6}$ g/cm$^3$ or $2 \times 10^{-6}$ moles/liter) and even less solubility in Ethanol. Zinc Oxide decomposes at $1975^0$C.

ZnO is a II-VI semiconductor with unique semiconducting, photoconducting, piezoelectric and optical properties. This combination of properties makes zinc oxide attractive for use in opto-electronic, electronic and sensor devices. ZnO-based thin films have many potential applications such as solar cells, displays, sensors (ref 1), photodetectors, light emitting diodes, laser systems (ref 3), solar window layers, surface acoustic-wave devices (ref 4), bulk acoustic-wave devices, short-wavelength semiconductor diode lasers (ref 10), and more.

### *Part a: ZnO Crystal Structures*

ZnO crystallizes in three forms – hexagonal Wurtzite, zincblende and cubic rock salt (see Figure 1). The predominant form is hexagonal Wurtzite since this structure is the most stable at ambient temperature and pressure. This hexagonal form has two interpenetrating sub lattices of $Zn^{2+}$ and $O^{2-}$ which make up the alternating basal planes. The zinc to oxygen coordination number is four with the cations surrounded by four anions in the corners of a tetrahedron and vice versa. The tetrahedral arrangement of atoms in the Wurtzite structure results is a non-centrosymmetric structure which gives rise to a dipole moment. This characteristic of zinc oxide Wurtzite is believed to be what gives rise to some of its unique properties such as piezoelectricity.

| Table 1: Physical Properties of ZnO | |
|---|---|
| Property (Ref 66, 15) | Value |
| Crystal structures | Wurtzite (stable at 300 K)<br>zinc blende<br>rock salt |
| Lattice parameters: $a_0$ | 0.32495 nm |
| $c_0$ | 0.52069 nm |
| $c_0 / a_0$ | 1.60 |
| Density | 5.606 g/cm$^3$ |
| Melting point | 1975 $^{o}$C |
| Thermal conductivity | 0.6, 1–1.2 |
| Linear expansion coefficient ( / $^{0}$C) | $a_0 : 6.5 \cdot 10^{-6}$ |
| | $C_0 : 3.0 \cdot 10^{-6}$ |
| Static dielectric constant | 8.656 |
| Refractive index | 2.008, 2.029 |
| Energy gap | 3.3 eV, direct |
| Intrinsic carrier concentration (per cm$^3$) | $10^{16}$ to $10^{20}$ |
| Exciton binding energy | 60 meV |
| Electron effective mass | 0.24 |
| Electron Hall mobility at 300 K for low n-type | 200 cm$^2$/V s |
| Hole effective mass | 0.59 |
| Hole Hall mobility at 300 K for low p-type | 5–50 cm$^2$/V s |
| Typical impurities | H, Al, In, Ga |
| Typical defects | Zinc interstitials, Oxygen<br>vacancies, zinc vacancies, complexes |

The hexagonal lattice constants are $a$ = 3.25 Å and $c$ = 5.2 Å. The ratio $c/a$ is about 1.60 which is close to the ideal value for a hexagonal cell i.e., $c/a$ = 1.633. Zinc oxide crystals exhibit several typical surface orientations. The most important surfaces are the basal plane, the prism plane, and the pyramidal plane crystal faces. Zinc ions are located on alternate basal planes to the oxygen ions. To achieve transparency and good conductivity the preferred crystal growth is in the (002) plane where atomic density is highest.

Zinc oxide may form the rock salt structure at relatively high pressures (ref 64). The rock salt structure is common for materials where the coordination number for the cations and the anions is six. A unit cell for the zinc oxide rock salt structure can be modeled with anions arranged on the face centered and corner sites of the cubic unit with one cation at the center of the cube and one centered on each of the 12 cube edges.

The zincblende structure can be formed when the crystal is grown on a cubic substrate. Like the rock salt structure, zincblende is a cubic crystal structure but the coordination number is four. This structure is characterized by two interpenetrating face centered cubic structures formed by the alternating anions and cations. A unit cell for this structure can be modeled with the anions occupying the face centered and corner sites of the cube and the cations occupying half of the tetrahedral positions (ref 76).

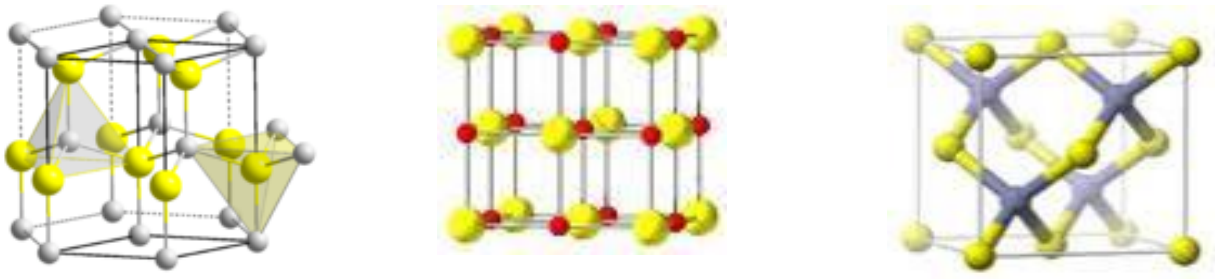

(a) (b) (c)

Figure 1: Zinc Oxide Crystal Structures

(a) Wurtzite, (b) Rock Salt, (c) zinc blende

***Part b: ZnO Electronic Properties for Renewable Energy Applications***

ZnO is a wide band gap, group II-VI semiconductor with a band gap of 3.3 eV at room temperature and a relatively high exciton binding energy of 60 meV (Ref 64). In its pure form, ZnO is an intrinsic n-type semiconductor with reported concentrations of about $10^{16}$ to $10^{20}$ per $cm^3$ in high quality material. The defect chemistry leading to the n-type properties results in nonstoichiometric ratios ($Zn_{1+\delta}O$ or $ZnO_{1-\delta}$, ref 19) according to the defect equations below (see Equation 1 and 2).

$$null \overset{ZnO}{\Longleftrightarrow} V_o^{oo} + 2e'' + O_o^x \quad (1)$$

$$null \overset{ZnO}{\Longleftrightarrow} Zn_i^{oo} + 2e'' + O_o^x \quad (2)$$

Doping that is n-type is generally achieved by substituting Zn with group-III elements such as Aluminum or Gallium according to Equation 3.

$$Al_2O_3 \overset{ZnO}{\Longleftrightarrow} 2Al_{Zn}^{o} + 2e'' + 3O_o^x \quad (3)$$

Reliable p-type doping with a range of materials has been attempted but remains a major hurdle to the full utilization of zinc oxide. The problem is twofold. First, the 'p type' dopants have low solubility in zinc oxide. Second, zinc oxide has a natural ability to override the p-type doping with impurities that bring about n-type properties. The elements that have been used as p-type dopants include group-I elements such as Li, Na, K (see Equation 4); group-V elements N, P and As (see Equation 5); and also to a lesser extent copper and silver.

Many of these elements form deep acceptors which do not produce significant p-type conduction at ambient conditions.

$$Li_2O \overset{ZnO}{\Longleftrightarrow} 2Li'_{Zn} + 2h^o + O_o^x \quad (4)$$

$$N_2O_5 \overset{ZnO}{\Longleftrightarrow} 2N'''_o + 6h^0 + 5O_o^x \quad (5)$$

The limited ability to achieve p-doping has restricted applications of ZnO in electronics and opto-electronics as a p-n junctions. Synthesizing p-type ZnO with good conductivity, mobility and stability is probably one of the greatest opportunities in the development area for ZnO.

***Part c: ZnO Optical Properties for Renewable Energy Applications***

The transparency of ZnO is due to the band gap (3.3 eV at 300 K) which makes this material transparent to light wavelengths greater than 400 nm, i.e., most of the visible and infrared range. The relatively large binding exciton energy facilitates applications of room-temperature exciton-based emitters and low threshold semiconductor lasers.

The fact that ZnO is both conductive and transparent puts it in an important class of materials called transparent conductive oxides, or TCOs. Today, the most important TCOs for renewable energy applications are Indium Oxide ($In_2O_3$), Tin Oxide ($SnO_2$), and Zinc Oxide (ZnO). These materials are typically doped using tin [($In_2O_3$):Sn = ITO], fluorine [($SnO_2$):F = FTO], and aluminum [(ZnO):Al = AZO], respectively.

***Part d: Other ZnO Properties for Sensor Applications***

Of the three materials mentioned earlier that are transparent conductive oxides, only AZO (i.e. zinc oxide that has been doped with aluminum) has piezoelectric properties. This property allows the material to generate an electrical charge when subjected to mechanical

deformation. Piezoelectric materials are believed to accumulate electrical charge because they have no crystalline center of symmetry.

The discovery of piezoelectric properties in ZnO led to applications in surface acoustic wave devices, bulk acoustic wave devices, acoustic-optic devices and short-wavelength semiconductor diodes. The piezoelectrical properties also have the potential for applications in renewable energy due to its ability to generate electrical charge when force is applied. Finally ZnO demonstrates ferroelectric properties when doped with transition and/or rare earth metals (Ref 63, 64). This makes it a candidate for spintronic devices.

## Section II: Applications and Opportunities for Zinc Oxide Thin Films in Renewable Energy Technology

### *Part a: Applications and Opportunities for Zinc Oxide Thin Films in Solar Cells*

Obtaining electrical power through solar technology is becoming increasingly desirable as electricity from conventional technologies becomes more expensive, less available and more harmful to the environment. Solar technology that produces electricity typically uses photovoltaic cells, also referred to as PV cells. The core of the PV cell is the semiconductor layers. These create a p-n junction which separates regions of electron generation from 'hole' generation. In other words, most of today's solar cells are really are just large area diodes. When sun light is absorbed into the diode layers, they have the unique ability to free electrons into the conduction band through the 'photovoltaic effect'. This is what ultimately will generate electricity (see Figure 2).

The so called 'first generation' PV solar cells used group IV elements like silicon. This technology used an expensive and laborious top down fabrication process. A perfect crystal of silicon that was about 3 X 0.3 meters was sawed and polished into 100 -200 micron thick wafers. The wafer production had to be done in a 'clean' high vacuum process because the slightest level of impurities would profoundly impact the conductivity of the material. There was a lot of material loss, the fabrication was a step-wise procedure, and the environmental conditions for processing the wafers were stringent. Bottom line, the first generations of solar cells were very expensive with over half of the solar module cost coming from the production of the silicon wafers themselves.

To address the cost prohibitive nature of these first generation solar cells, thin film solar cells were developed. These use far less material and often can be synthesized in open air environments. The semiconductor material used in thin film solar cells is frequently silicon but instead of crystalline silicon, amorphous silicon is used which brings the cost down appreciably. Other semiconductor materials are also increasingly being used such as Cadmium Telluride (CdTe) and CIGS – a composite of Copper, Indium, Gallium and Diselenide.

What all of the solar cell technologies have in common is an ability to produce the 'photovoltaic effect'. As mentioned earlier, this means they can absorb light and convert it to electricity. These semiconductor materials produce the 'photovoltaic effect' because they have a relatively small energy gap between electrons in the valence band and the conduction band. The band gap is small enough that when a photon of sunlight is absorbed into the semiconductor layer, the energy is sufficient to elevate a valence electron into the conduction band. The band gaps for these semiconductor materials are typically in the 1 to 2 eV range.

In addition to the semiconductor layers, the typical photovoltaic cell is composed of a glass or plastic layer that protects the cell from the external environment and a metal back contact. There is also a layer called the antireflective coating and one that is called the window layer. The window and antireflective layer functions may be accomplished within one layer of the solar cell.

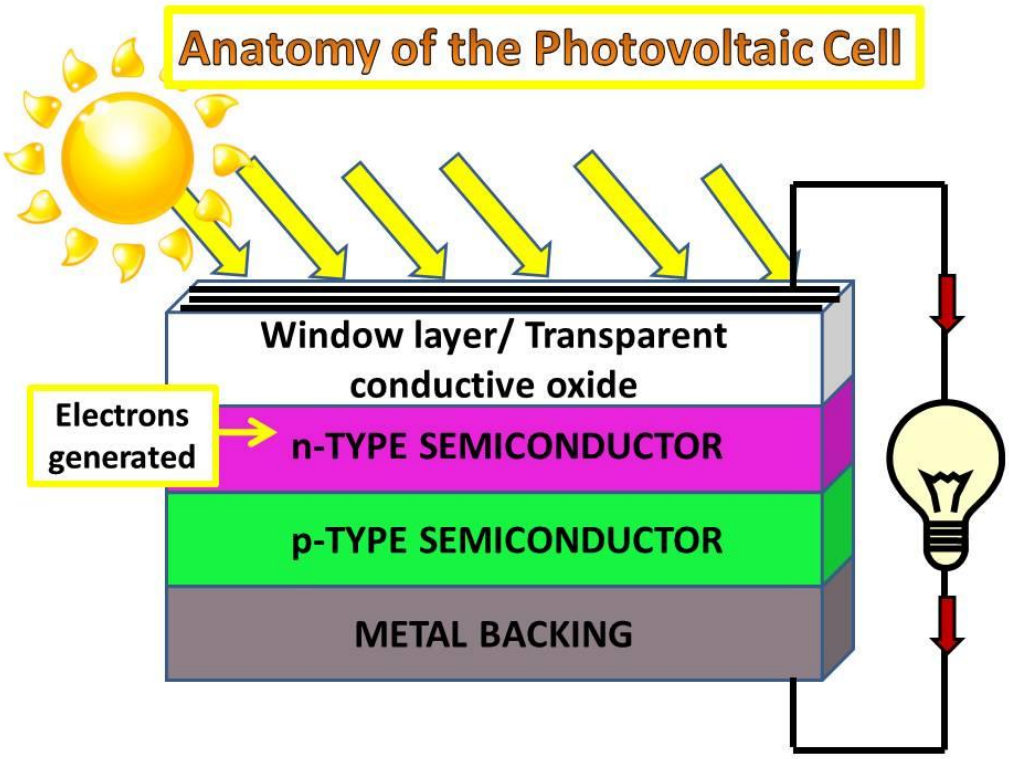


Figure 2: Anatomy of a PV Solar Cell

### i. Window layer

Since the source of power for solar cells is the electrons being generated by the absorption of sunlight, it is essential that the negatively charged electron be removed before it is able to recombine with the positively charged hole it has left behind. A conductive metal might be the obvious material for this function but metal would interfere with the incoming sunlight, thus reducing the 'photovoltaic effect'. Glass or plastic materials could be used to transmit the solar rays but these materials will not conduct electricity. The window layer performs both functions of transmitting the sunlight and collecting the electrons being generated by the core semiconductor layers. The window layer ensures that the maximum number of electrons are extracted while also maximizing the sunlight that is transmitted to the semiconductor layers of the solar cell. The 'window layer' is usually made up of transparent conductive oxides (TCO's).

### ii. Antireflective layer

The 'window layer' may also double as an antireflective layer if it is used to reduce the reflection of sunlight from the surface of the solar cell. When light shines on a solar cell, it may be reflected, absorbed, or transmitted. Only when the light is absorbed into the semiconductor material can it undergo the 'photovoltaic effect' to generate electricity. If light is reflected, the 'photovoltaic effect' simply will not occur and power is lost. Therefore the antireflective layer should maximize the transmission of sunlight over the entire solar spectrum and over the sun's incident angles and minimize the reflectance of this light (see Figure 3). Since the inner semiconductor layers may be shiny, the antireflective layer can have a significant impact on the energy output.

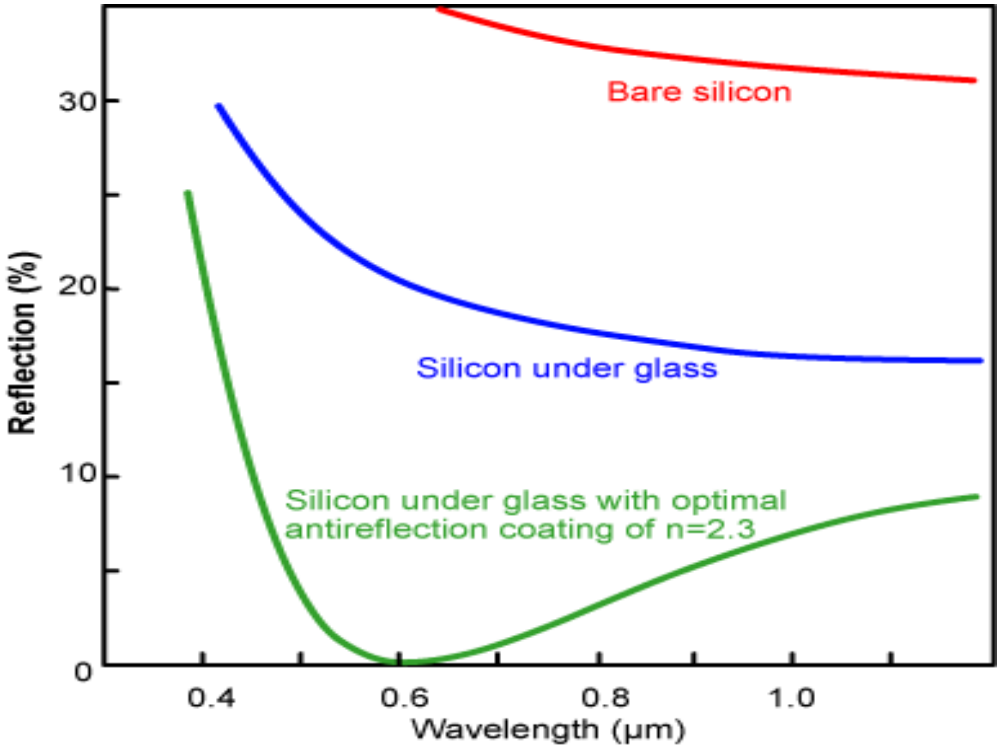


Figure 3: Antireflective Layer

The thickness of the anti-reflection coating is chosen so that the wavelength in the coating is one quarter the wavelength of the incoming wave. This will produce interference such that the wave reflected from the top surface of the antireflective coating is out of phase with the wave reflected from the top of the semiconductor surface. These out-of-phase reflected waves destructively interfere with one another resulting in zero net reflected energy (ref 38).

The window/antireflective layers are often made with Tin-Doped Indium Oxide (ITO). This material is relatively expensive due to the high cost and limited supply of indium. Also, more stringent processing conditions are needed to make ITO films which further increase the cost. Zinc Oxide makes a good replacement for ITO because it is a less expensive with good semiconductor properties and good transparency. In addition to having a relatively low material cost, zinc oxide is attractive because there is more flexibility in processing options.

***Part b: Applications and Opportunities for Zinc Oxide in Dye Sensitized Solar Cells***

The dye sensitized solar cell (DSSC) technology is another source of clean and renewable energy. The excitement around this technology vs. conventional solar cell technology stems primarily from the fact that it is so inexpensive and simple in design. The technology is not particularly energy efficient but progress is being made in improving efficiencies through advances in material science. Zinc oxide shows the potential to be a good electrode material for dye sensitized solar cells (DSSC) - either in conjunction with or as a replacement for the prevalent electrode material in DSSC's i.e., titanium dioxide.

The conversion of sunlight into electricity follows a somewhat different path in the DSSCs (see Figure 4). First, organic dyes are the medium for capturing light. This means that expensive semiconductor materials are not needed. Instead, inexpensive materials that are easily processed by a wide range of methods may be used. Also, the dye may be chemically tailored to capture the full range of the solar spectrum whereas the semiconductor materials used in conventional solar cells are limited to the light spectrum that excites the band gap energy.

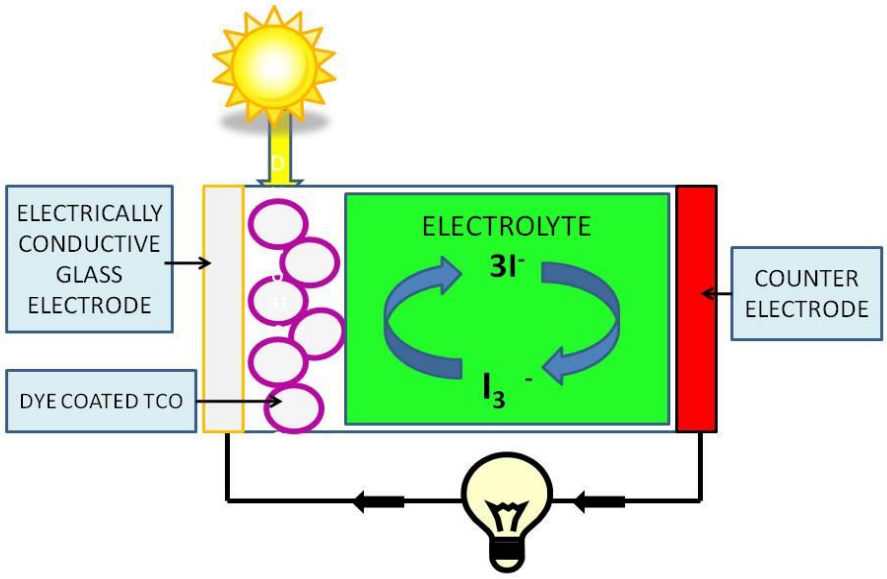


Figure 4: Diagram of a DSSC

The dye sensitized solar cell is a bit like a cross between a battery and the solid state solar cells described earlier. As with a battery, the DSSC has electrolyte and electrodes where charge transfer takes place. And as with a solar cell, there is the formation of an excited state that can be converted to electron-hole pairs.

In the DSSC, an exciton is produced when the dye absorbs sunlight which is a tightly bound electron-hole pair. The electron must be dissociated from the hole for charge generation. Exciton dissociation takes place at the interface between the dye and the transparent conducting oxide. The following steps describe the mechanisms that take place in the DSSC:

1. Photon Absorption and exciton formation

   $$\text{Dye} + \text{photon} \rightarrow \text{Dye}^*$$

2. Exciton charge dissociation

   $$\text{Dye}^* + \text{ZnO} \rightarrow \text{Oxidized Dye} + \text{ZnO}'$$

3. Charge transport

   $$\text{ZnO}' \rightarrow \text{ZnO} + e^- \qquad \text{(to anode)}$$

4. $$\text{Oxidized Dye} + {}^3/_2\ I^- \rightarrow \text{Dye} + \tfrac{1}{2}\ I_3^- \qquad \text{(electrolyte)}$$

   $$\tfrac{1}{2}\ I_3^- + e^- \rightarrow {}^3/_2\ I^- \qquad \text{(to cathode)}$$

Light absorption is performed by a single layer of dye, usually a ruthenium-based organic compound that is chemically attached to the rough surface of a layer of interconnected conductive metal oxide such as zinc oxide or titanium oxide. Titanium Dioxide ($TiO_2$) is the most widely used transparent conductive oxide being used in DSSCs today. However, ZnO is being considered as a replacement for $TiO_2$ because it has many similar properties – e.g. transparency and band gap – and it has some advantages. ZnO has better electron mobility than $TiO_2$. Also, there are a lot more options and flexibility for synthesizing ZnO nanostructures. This opens up many design possibilities for improving the DSSC. Thus, ZnO is increasingly being looked at as a standalone electrode material or in combination with $TiO_2$.

In the DSSC, the TCO particles, e.g., zinc oxide or titanium dioxide, are typically nanocrystals to provide a support structure for the dye molecules as well as to facilitate charge transfer. The dye, ruthenium-polypyridine, works somewhat like the photosynthesis process that takes place in plants. In fact, the dyes used in educational experiments are often a berry extract. The molecules of dye, once they have been excited by light, are able to transfer an electron to the semiconducting electrode layer i.e. zinc oxide, via a process called electron injection or sensitization.

The positive charge is transferred from the dye to a mediator that is an electron donor present in the electrolyte. The oxidized mediator brings the positive charge from the dye to the opposite side of the cell which is called the counter electrode. The electrons are collected at the TCO electrode side then travel through an external circuit to the 'counter electrode' and the mediator ($I_3^-$) is returned to its original reduced form ($I^-$). The circuit is thus closed and electricity is produced.

Due to their simple construction, the new cells offer the hope of a significant reduction in the cost of solar electricity. The efficiencies are very low because there are losses in each phase of the process. The losses result from a multitude of material issues. Advances in material science around all the components such as the zinc oxide electrode may be the key to making this technology viable.

***Part c: Other Applications and Opportunities for Zinc Oxide Thin Films as Sensors***

Beyond renewable energy, zinc oxide thin films have received much attention for a wide range of sensor applications. The sensor mechanism broadly involves the absorption of whatever is being detected onto the surface of the zinc oxide structure. The absorption results in changes in the properties of the zinc oxide. Because absorption is fundamental to the detection of a substance, thin films and nanostructures of ZnO can achieve a higher level of sensitivity compared to bulk because they have a higher ratio of surface area to total volume. Consequently, the synthesis of ZnO thin films has great promise for sensor applications.

Potential zinc oxide sensor opportunities include gas sensors, force sensors, humidity sensor, light sensors, electrochemical potentiometric nanosensors, pH sensors and biosensors

(Ref 1-15, 63). Zinc oxide is most commonly used to detect gases. The mechanism for detection involves the gas being absorbed on the surface of the zinc oxide. This in turn brings about changes the surface resistance of the zinc oxide due to the oxidizing properties of the target gas according to the defect equation and variations on these as discussed earlier (ref 59, 69). A range of dopants can be used to alter the sensitivity that zinc oxide has for a particular material.

Zinc oxide can also be used as a force detector because it generates a current under mechanical force due to its piezoelectric properties. As a light sensor the zinc oxide would be designed much like a DSSC, with a light absorbing dye that injects charge into a zinc oxide thin film.

**Section III: Scope of Zinc Oxide Thin Film Sol-Gel Research**

Zinc Oxide, a material already widely used in opto-electronic, electronic and sensor devices, is increasingly gaining importance in emerging renewable energy technologies. The reason behind the growing interest in Zinc Oxide is the material's rather ideal combination of chemical, mechanical, and electrical properties as well as its ease of processing, cost effectiveness, and low toxicity. Zinc Oxide is a wide band gap (3.3 eV) semiconductor with a high exciton binding energy (60 meV) and good conductive properties when doped with materials such as Group III elements such as Aluminum and Gallium. In addition, when processed properly, it is transparent and can be easily synthesized into many types of nanostructure such as nanoflowers, nanorings, nanowires, nanotubes, nanoparticles, quantum dots and, of course, nanosheets or thin films (Ref 64). The promise of using Zinc Oxide to make effective and cost efficient solar cells has intensified research efforts in this area.

One of the approaches to synthesize Zinc Oxide structures is the sol-gel process. The sol-gel process gets its name from the fact that the process starts with a solution of the precursor ingredients which is slowly gelled and then solidified into some final ceramic material. This process is a wet-chemical technique that is widely used to make ceramic materials. It is cost effective and simple, utilizes ambient and/or 'in air' conditions and uses relatively inexpensive precursor materials when compared to other ceramic processing techniques. In addition the sol-gel approach gives good control of chemical composition and morphology and can be used to cover large surfaces.

The sol-gel process has been shown to successfully make good Zinc Oxide thin films and Zinc Oxide nanostructures. In the Zinc Oxide thin film sol-gel reported in literature, organic solvents have almost exclusively been used. The structures produced with these sol-gels were analyzed for composition, physical and electro-optical properties. The published reports indicate, through characterization of crystal structure and optical transparency, that the sol-gel process is a viable fabrication method for mass production of good Zinc Oxide thin films and nanostructures.

The research described here builds on the work that has been reported on Zinc Oxide sol-gel thin film fabrication. The objective of this research will be to:

- Evaluate the synthesize methods for making Zinc Oxide thin films that have been reported in literature. Specifically, the reported sol-gel process steps reported will be duplicated and assumptions tested around the key process conditions such as:

    a. The type of precursor materials to use.
    b. Concentration of precursor materials.
    c. Feasibility of simple substrate e.g. microscope slides.
    d. Feasibility of simple film fabrication methods e.g. a one step, scalable processes.

- Produce Zinc Oxide films using a modified sol-gel process that is based on water as the primary solvent.
    a. Identify process parameters for stable aqueous sol-gel.
    b. Identify process parameters for good film formation with aqueous sol-gel.

Chapter 1 of this report discussed general background pertaining to Zinc Oxide as well as ZnO thin film applications for renewable energy applications and sensors. In the following chapters, the research done in this body of work will be presented in great detail. Chapter 2 presents an extensive review of the current technology for Zinc Oxide thin film fabrication. Chapter 3 will address the first objective concerning the fabrication of Zinc Oxide thin films using organically based sol-gels. Chapter 4 will address the second objective concerning the fabrication of Zinc Oxide thin films using water based sol-gels. Chapter 5 will provide results from the characterization of the Zinc Oxide thin films via UV-Vis spectrophotometry. Chapter 6 will explore the mechanistic understanding of the sol-gel process and presents sol-gel thin film characterization via Raman spectrophotometry. Finally, Chapter 7 will summarize conclusions about the research and will present thoughts for future research consideration.

# Chapter 2: Technology for Zinc Oxide Thin Film Fabrication

## Section I: Overview of Thin Film Technology

A 'thin film' is defined as a film of material, often a ceramic material, that is nanometers to micrometers thick. Thin films are applied to devices when a smaller and/or thinner amount of material enables the same or better performance. Advances in fabrication and characterization methods of these microscopic structures have brought about a surge in thin film research and development.

Broadly speaking, 'thin films' are developed through either physical or chemical deposition onto a solid substrate. **Physical deposition** uses mechanical or thermodynamic means to produce a thin film of solid and includes techniques such as sputtering and pulsed laser deposition. Thermal evaporation is also a form of physical deposition and includes a more sophisticated process called molecular beam epitaxy.

**Chemical deposition** involves a chemical change to the precursor to produce the thin film. Chemical deposition may use a liquid precursor, in which case the method is called chemical solution deposition (CSD). Alternatively, the deposition method may use a gaseous precursor, in which case the method is called chemical vapor deposition (CVD).

The chemical solution deposition method (CSD) is commonly referred to as the sol-gel method. As mentioned earlier, the sol-gel fabrication technique is distinguished by its liquid precursor. The sol-gel technique involves condensing a liquid to a gel network of integrated, cross linked microparticles. Then the so called gel is further condensed and thermally treated to the final ceramic material (see Figure 5). The sol-gel process allows the scientist to make a good ceramic material with tailored electrical, optical or other properties from a wet chemical method that requires simple equipment and accommodating synthesis conditions.

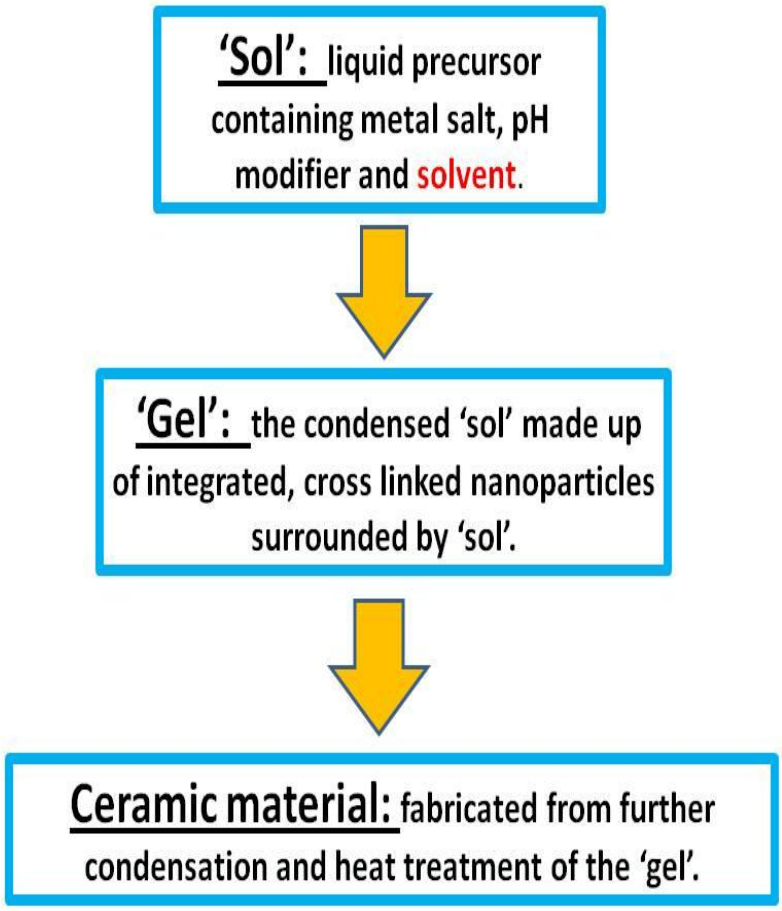


Figure 5: Sol-Gel Process

The sol-gel method has many advantages over other thin film techniques in that it is simple and easy, it is cost effective in both materials and energy used, it does not require special templates, it can be used to cover very large areas with good uniformity of film thickness and microstructure, and it does not require stringent process conditions. Beyond these, sol-gel techniques have advantages for controlling the microstructure of the films and it allows easy doping of the crystal for targeting specific optical and electrical properties.

The initial sol-gel solution usually contains an organo-metal compound, a solvent and a pH modifier. The metal compound undergoes hydrolysis and polycondensation creating a

cross linking from metal ion to oxygen ion or metal ion to hydroxide ion depending on the pH used for the reaction.

As the liquid is evaporated, a gel forms and a matrix takes shape that could be described as a continuous solid skeleton with a liquid/gel phase filling the pores between the solid particles. The liquid/gel phase is gradually removed leaving behind a 'solid skeleton'. This structure is then annealed at high temperatures to create the final desired ceramic material.

**Section II: Zinc Oxide Thin Film Technology**

ZnO thin films are being widely researched as a result of their usefulness in emerging renewable energy and sensor applications. In the renewable energy area, ZnO thin films are showing promise as window layers, antireflective layers, and electrode materials. If there is a fabrication method for thin films, it has likely been studied for fabricating Zinc Oxide thin films. For example, recent reports have been published of studies where Zinc Oxide thin films were made via molecular beam epitaxy (52), dc and rf sputtering (53, 59), chemical vapor deposition (55), metal-organic chemical vapor deposition (57), pulsed laser deposition (58), spray pyrolysis (56) and of course sol-gel (1-15). Some morphological images of zinc oxide fabricated by molecular beam epitaxy (ref 53) with good results are shown below in Figure 6.

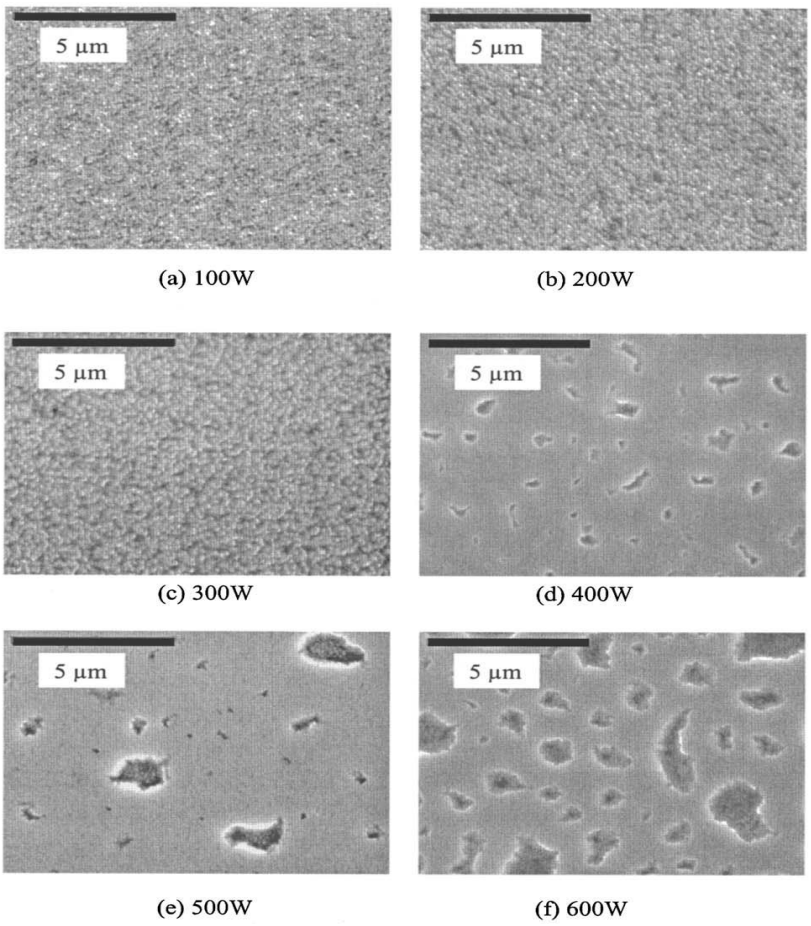


Figure 6: SEM images of ZnO Fabricated by Molecular Beam Epitaxy

(Shown are films from various rf powers (watts) from Ref 53)

**Section III: Zinc Oxide Sol-Gel Thin Film Technology**

To capture the current 'state of the art' Zinc Oxide sol-gel methodology, an extensive review of publications (Ref 1 -15) on this topic was undertaken. The reported studies were scrutinized for optimal processing conditions based on the criteria that the films formed were:

1. Free of visible physical defects such as cracks and pin holes.
2. Had crystal orientation in the (002) direction, that is, the c-axis of the Zinc Oxide Wurtzite structure was parallel to the normal of the substrate plane.
3. Optical transmittance of 80% or more based on zinc oxide sol-gel literature reports (Ref 1-15) as benchmarks for transparency given a film thickness in the range of 200 to 400 nm.

Some morphological data was given in several of the studies which indicated the quality of the films as described above (see Figure 7). Although the studies provided guidance in selecting process conditions, there was very little explanation as to why these conditions were important. Generally the studies reported the effect of a process variable on film characterization and by this determined which condition satisfied the film criteria outlined above.

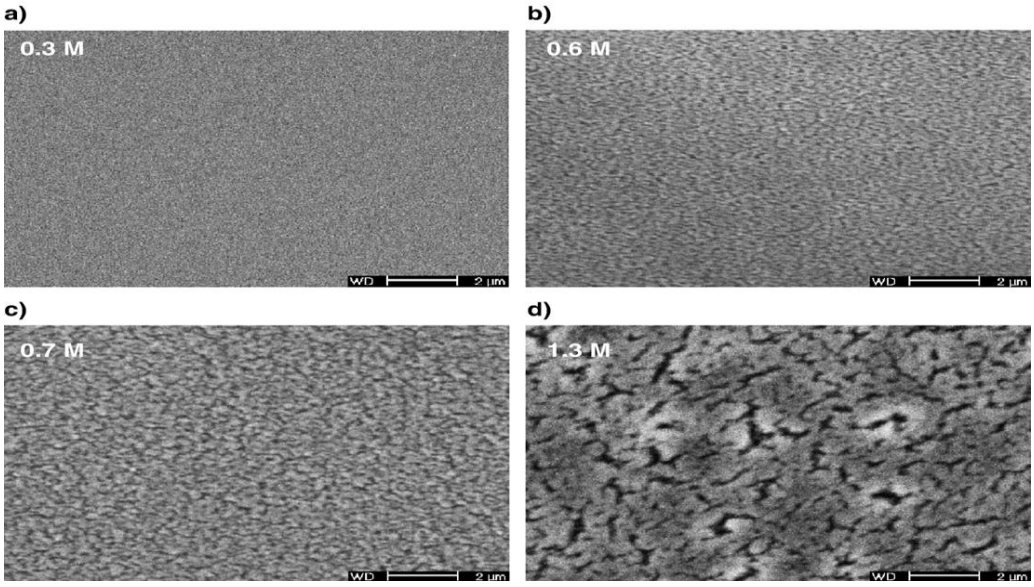


Figure 7: SEM micrographs of ZnO films prepared by Sol-Gel

The following summarizes findings from these reports:

1. **Zinc Acetate Salt:** The most commonly used precursor zinc salt was Zinc Acetate Dihydrate. Other zinc salts such as zinc nitrate and zinc perchlorate have been looked at (ref 10) but were reported to be **incapable** of forming sols and/or the results were **not** reproducible. This reference proposed that the acetate group was a key part of the Zinc Oxide sol-gel chemistry and film development stating, 'Acetate plays an important role in sol formation, by complexing Zn(II) cations, in competition with the MEA. Two alternative hypotheses can be formulated. According to the first one, acetate can form Zn(II) complexes on the particle surface, hindering the growth process. … Indeed, initial films are formed by zinc oxo-acetates'. Other reports are consistent with this (Ref 5, 6, 30) and describe a similar hypothesis with the chemistry depicted in Figure 8. Based on these reports, zinc acetate was chosen for the research reported here.

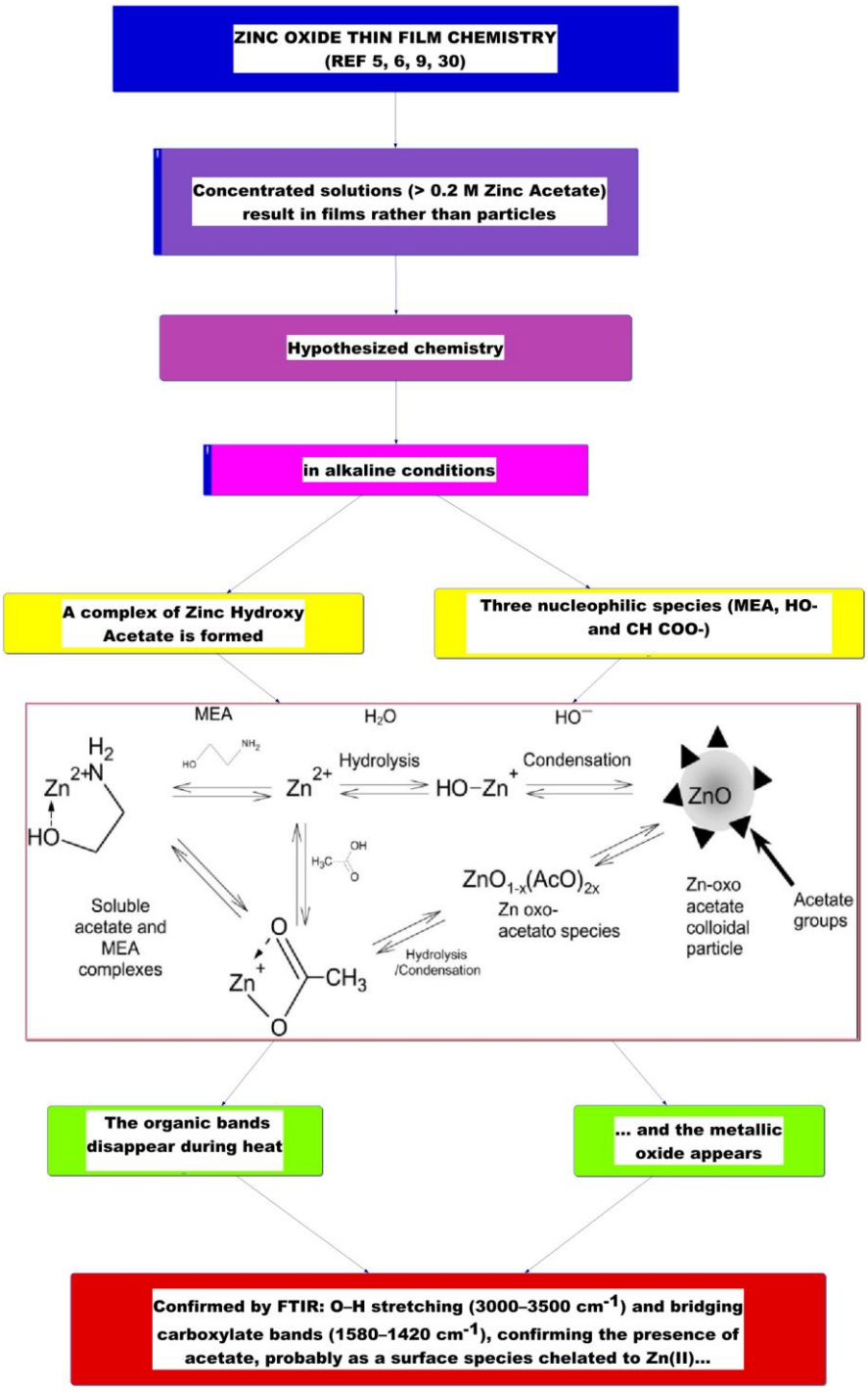


Figure 8: Zinc Acetate Sol-Gel Chemistry

2. **Concentration of Zinc Salt:** The concentrations of zinc salt in the published references ranged from 0.02 to 2.3 M (moles per liter) zinc salt in solvent. Concentrations of 0.3 M to 0.75 M were found to produce acceptable films in the various organic solvents. Concentrations that were low (e.g., less than 0.2 M) did not yield films with good c-axis orientation, meaning that the c-axis of the hexagonal Wurtzite crystal structure was not parallel to the normal of the substrate. Concentrations that were excessively high (e.g. 1.3 M IPA [ref 1], 2.3 M [ref 8]) resulted in reduced clarity and/or c-axis orientation. One study worth noting looked at a range of zinc acetate concentrations and found a range of 0.3 to 0.6 molar produced good films (See Table 2).

Table 2: Zinc Oxide Sol-Gel Literature Reports on Zinc Acetate Concentration

| Reference Cited with * = Best results | 1 |
|---|---|
| Molar Ratio of Zinc Acetate to MEA | 1:1:(used anhydrous Zinc Acetate) |
| Solvent | IPA |
| Zinc Acetate Concentration (moles/liter) | 0.3*, 0.5*, 0.6*, 1.3 |
| Transparency (% Optical Transmittance > 80) | Yes |
| (002) orientation | yes |

3. **pH Modifier**: The pH is important in the formation of metal sol-gel complexes. The type and level of pH modifier can be important. Several types of pH modifiers have been reported in Zinc Oxide sol-gel including Monoethanolamine (MEA), Triethanolamine and Lactic Acid. MEA was the most frequently used pH modifier/complexing agent. It was shown repeatedly to produce good Zinc Oxide thin films. In contrast, less c-oriented films were reported when Triethanolamine and Lactic acid were used. The level of pH modifier is also important. At least a one to one ratio of zinc salt to pH modifier was reported to be necessary for acceptable thin film fabrication. One literature report (see Table 3) evaluated a range of MEA concentrations and confirmed that a 1:1 molar ratio of MEA to zinc acetate was optimal for Zinc Oxide thin film fabrication.

Table 3: Zinc Oxide Sol-Gel Literature Report on pH Modifier Level

| Reference Cited with * = Best results | 5 |
|---|---|
| Molar Ratio of Zinc Acetate to pH modifier | 1:0 ; 1:0.25 ; 1:0.5 ; 1:0.75 ; 1:1* |
| Solvent | Methanol |
| Zinc Acetate Concentration (moles/liter) | 0.6 |
| Initial dry temperature ($^0$C) | 300 |
| Initial dry time (minutes) | 10 |
| Annealing temperature($^0$C) | 600 |
| Annealing time (hours) | 1 |
| Film substrate | Glass |
| Transparency (% Optical Transmittance > 80) | Yes |
| (002) orientation | Yes |

4. **Organic Solvents:** A range of solvents have been reported, all showing the ability to produce good films. The most frequently used solvents were organic liquids such as Methanol, Ethanol, and Isopropanol (IPA), n-Butanol or 2-Methoxyethanol (MOE). All five have been reported to produce films with the desired preferential crystal orientation and optical transparency. However, one study (ref 10) found **MOE** allowed more preferential crystal orientation during heat treatments than sols made with **Ethanol**. The hypothesis put forth by the investigators was that the higher boiling point of MOE was a key factor stating "The initially formed Zn-oxo acetate gel can rearrange in a more complete fashion in the presence of 2-ME (MOE), due to the presence of solvent until relatively high temperatures, during the deposition-thermal cycles (b.p. of 2-ME = 125 $^{0}$ C). Quick evaporation of a volatile solvent such as Ethanol (b.p. = 78 $^{0}$ C) leads fast to a dried set of agglomerated particles, which might not develop a definite orientation (random nucleation being more probable for smaller particles)." Despite this information, the optimal organic solvent was not clear since many organic solvents have been reported and no study has comprehensively reviewed how these solvents compare.
5. **Mixing of Solution:** There was a wide range of mixing conditions used. Several studies simply reported to 'stir until a clear, homogenous solution is formed'. The time used to mix the solution ranged from 30 minutes to 2 hours. The temperatures ranged from room temperature to 100 $^{0}$ C. Of course, the temperature would depend on the solvent but there was no clear cut picture of how much time was needed to ensure the metal cross linking had been established or if any time was needed at all. Similarly, in some of the studies the solutions were given time to 'age'. It was not reported whether this had any benefit. Although the optimal mixing time was not clearly indicated, a mixing time of 2 hours at 50 to 80 $^{0}$ C (depending on solvent boiling point) appeared to ensure good 'sol' microstructure development.

6. **Film formation process**: Spin coating was the method most frequently reportedly used to form films. Often the deposition/spin coating step was repeated 6 to 10 times to get a film thick enough for analyses. This approach was not used in this research for two reasons. First, because the spin coat process required repeated steps, there was unnecessary complexity being designed into the process which could lead to poor cost effectiveness and reproducibility. Second, spin coating is not easily scalable for commercial use. For these reasons spin coating was deemed unsuitable for meeting the original goals of this project. A more simple approach was used as will be discussed in future chapters.
7. **Film Substrate**: A variety of substrates were reported including glass, quartz, sapphire, and silicon. Substrates such as sapphire that have a somewhat better crystal match to Zinc Oxide Wurtzite tended to show better film crystal orientation (See Table 4). Similarly, putting a seed layer on the substrate would result in better crystal orientation (ref 13). However, given thick enough films and/or the right thermal treatment, all substrates had the potential to yield acceptable crystal orientation and optical transmittance.

Table 4: Zinc Oxide Sol-Gel Literature Reports on Film Substrate

| Reference Cited with * = Best results | 2 | 8 |
|---|---|---|
| Molar Ratio of Zinc Acetate to MEA | 1:1 | 1:1 |
| Solvent | MOE | n-Propyl alcohol |
| Zinc Acetate Concentration (moles/liter) | 0.5 | 2.3 |
| Initial dry temperature ($^0$C) | 350 | Humid air |
| Initial dry time (minutes) | 15 | 10 |
| Annealing temperature($^0$C) | 500 | 450 |
| Annealing time (hours) | ½ | NA |
| Film substrate | Glass, quartz and sapphire* | Soda glass, silicon wafers, KBr single crystals |
| Transparency (% Optical Transmittance > 80) | Yes | Yes |
| (002) orientation | yes | No |

8. **Drying Process**:

The successful transformation from solution to gel to acceptable ceramic material is extremely dependent on the drying process. For ZnO there are several temperatures that are crucial to film formation as shown in Figure 9.

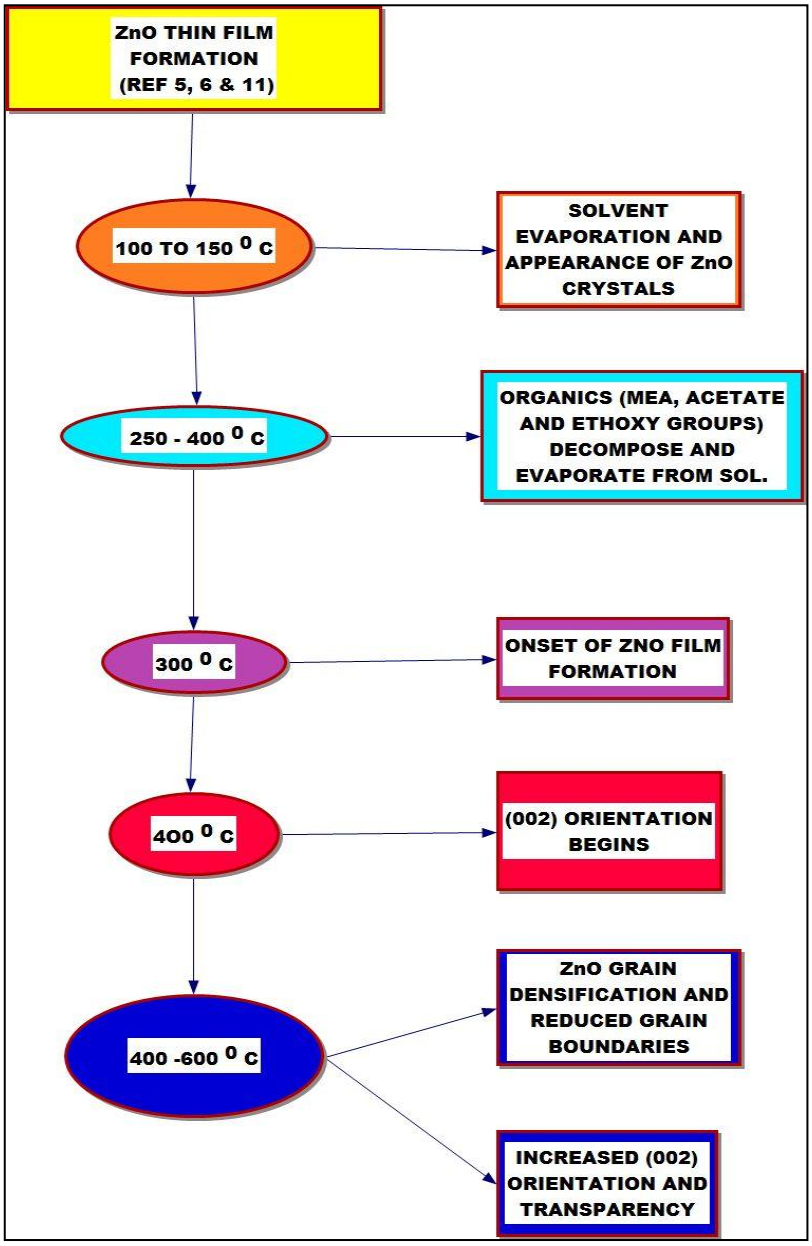


Figure 9: Thin Film Formation Steps

The ZnO sol-gel must be dried at a high enough temperature to remove solvent and other organic compounds but not so high that the film begins to degrade. The rate of drying is also important and dependent on the kinetics of the mass transfer of precursor materials out of the sol-gel as well as the formation of the optimal crystal structure. A drying rate that is too rapid might result in film defects and/or no film at all. A drying rate that is too slow might be unnecessarily costly.

Zinc Oxide thin film drying processes were generally separated into two stages: an initial drying step and a final annealing step. The two steps were mostly needed because of the repeated nature of the spin coat process that was described earlier.

**Initial Drying Step:** This initial drying was generally used in procedures that required repeated application of the sol – procedures such as spin coating. The 'initial drying' resulted in the removal of the solvent phase and some of the organics since the MEA and acetate groups decompose at 200-400$^0$C. There were several studies that looked at the initial drying time (See Table 5). As can be seen, no conclusive evidence could be drawn from this as to the best drying temperature.

Table 5: Zinc Oxide Sol-Gel Literature Reports on Initial Drying Temperatures

| Reference Cited with * = Best results | 6 | 13 |
|---|---|---|
| Solvent | Methoxyethanol | Methoxyethanol |
| Zinc Acetate Concentration (moles/liter) | 0.35 | 0.5 |
| Initial dry temperature (0C) | 150, 250 , 350* | 400, 500, 600* |
| Initial dry time (minutes) | 10 | 10 |
| Annealing temperature(0C) | 700 | 600 |
| Annealing time (hours) | 1 | 1 |
| Transparency (% Optical Transmittance > 80) | Yes | Yes |
| (002) orientation | Yes | Yes |

**Final Annealing Process**: Following the drying step, an annealing step was done at 400-600$^0$C to remove any residual organics as well as to dehydrate zinc hydroxide to form the final Zinc Oxide film according to Equation 6.

$$Zn(OH)_2 \rightarrow ZnO + H_2O \qquad (6)$$

There were several studies that looked at annealing temperature (see Table 6). Based on these studies, the best results for film formation appear to be anywhere from 500$^0$C to 600$^0$C.

Table 6: Zinc Oxide Sol-Gel Literature Reports on Annealing Temperatures

| Reference Cited with * = Best results | 3 | 4 | 7 | 11 | 12 |
|---|---|---|---|---|---|
| Solvent | MOE | Methanol | IPA | Ethanol | MOE |
| Zinc Acetate Concentration | 0.75 | 0.02 | 0.3 | 0.4 | 0.5 |
| Initial dry temperature ($^0$C) | 300 | 80 | 250 | 300 | 300 |
| Initial dry time (minutes) | 10 | 10 | 5 | Not Reported | 10 |
| Annealing temperature($^0$C) | 400,500, 600* | 500, 525*, 550, 575 | 300,400, 500* | 400, 450, 500, 550*, 600 | 400,500, 600*, 700 |
| Annealing time (hours) | Not Reported | ½ | 1 | Not Reported | 1/2 |
| Transparency (% Optical | Yes | Yes | Yes | No (70%) | Not reported |
| (002) orientation | Yes | Yes | Yes | Yes | Yes |

To summarize, the sol-gel fabrication approach is capable of making high quality zinc oxide thin films which are free of defects, have good crystal development with c-axis orientation and which are more than 80% transparent. The conditions which have been shown to produce this are as follows:

1. Metal salt: The use of Zinc Acetate (usually the dihydrate form) as the metallic salt.
2. Concentrations: A concentration between 0.3 to 0.6 molar Zinc Acetate in solution results in better crystal structure..
3. pH: An alkaline pH using Monoethanolamine (MEA) in a 1:1 molar ratio with Zinc Acetate.
4. Solvent: An organic solvent but without a clear conclusion as to which is best since reports of Methanol, Ethanol, Isopropanol, n-Butanol and 2-Methoxyethanol have all been shown to yield good zinc oxide films.
5. Mixing conditions: Mixing in the range of 50 to $80^0$C for about 2 hours – though no clear cut study was done to truly evaluate this.
6. Film Synthesize: Fabrication of films in a series of cycles using spin coating, which is complex and not easily scaled to commercial use.
5. Substrate: the crystal orientation of the zinc oxide films will develop c-axis orientation more readily on substrates that have a closer match to the Wurtzite hexagonal crystal structure but given a film thickness of 200 to 300 nm other substrates that have a poor match such as glass can produce acceptable films.
6. Drying process: A two-step drying process was generally used with the final annealing temperature ideally being in the 500 to $600^0$C range.

# Chapter 3: Fabrication of ZnO Thin Films Using Organic Based Sol-Gel

The objective of this research was to reproduce the work done in previously reported studies and to explore assumptions reported around the key process conditions. A variety of different synthesis conditions were evaluated including: the type of precursors used, concentration of precursor used, the feasibility of simple substrate i.e. microscope slides and the feasibility of a one-step film formation method. Also pursued through this work was a mechanistic understanding of the Zinc Oxide sol-gel process.

## Section I: Identification of Key Factors Controlling Organic Based ZnO Sol-Gel

In this section, the research focus was on an initial assessment of ZnO sol-gel processes using organic solvents. The identification of key process conditions was based on the variables outlined in the last chapter. Two solvents were used initially: Isopropanol (IPA) and 2-Methoxyethanol (MOE). These were chosen because they were frequently reported in literature to produce good Zinc Oxide thin films. Also they represented a nice range of boiling point and hydrophobicity behavior.

The basic process steps are outlined in Figure 10. A 0.5 molar solution of zinc acetate dihydrate (Alfa Aesar, 98 – 101%) was made in 30 ml of solvent. The solvents, as mentioned earlier, were IPA (Sigma Aldrich, USP Grade) and MOE (Sigma Aldrich, 99% or greater, Reagent Plus Grade). Monoethanolamine (Sigma Aldrich, 99% or greater) was added in a 1:1 molar ratio to the Zinc Acetate Dihydrate. The ingredients were weighed carefully and then added to a glass beaker that had been cleaned with hot soapy water followed by distilled water. The solution was stirred using a magnetic stirrer on a hot plate and kept at 60 - $80^0$C for 2 hours. Using these conditions, clear, homogeneous sols were made with both solvents. The MOE sol had a bright yellow color whereas the IPA sol was colorless. Both sols were water thin.

Films were prepared by placing one drop of the sol onto a glass microscope slide using a pipette. The droplet spreads out into a thin film through capillary action. The thickness of the film is calculated to be approximately 400 nanometers thick based on the volume of the sol placed on the slide (1 droplet equal to 1/20 ml), the area covered (approximately 0.3

square centimeters), the concentration of the sol (0.5 moles/liter), zinc oxide molecular weight (81 g/mol) and the density of zinc oxide (5.06 g/$cm^3$). This is in the range of thickness that was obtained in literature reports which reported films that were 200 to 400 nanometers thick.

The films were allowed to dry in air overnight. After one day, the Methoxyethanol film was visually transparent and free of cracks and pin holes whereas the IPA sol was not clear or was not free of visual defects such as holes and cracks.

The two sols were stored for 3 months. At the end of this time the sol based on IPA was showing signs of degradation with evidence of cloudiness in the solution. The MOE sol, however, was still clear and homogenous with the same yellow color.

A film was made with the MOE sol at this time – again on a glass microscope slide. One drop of sol was used and the film was allowed to dry in air overnight. Then the film was first dried at $300^0$C for ten minutes to remove any remaining solvent followed by $600^0$C for 1 hour. The rate of heating the furnace was $5^0$C/min. The film was allowed to cool in the furnace. The resulting film was visually transparent and free of cracks or pin holes.

These initial exploratory series of experiments confirmed that the process being used was capable of making films. In addition, it was clear that solvent was a key variable in the final properties of the Zinc Oxide thin films. Importantly, solvent has not been a variable that had been reported with any detail as to its impact on making good Zinc Oxide thin films using sol-gel.

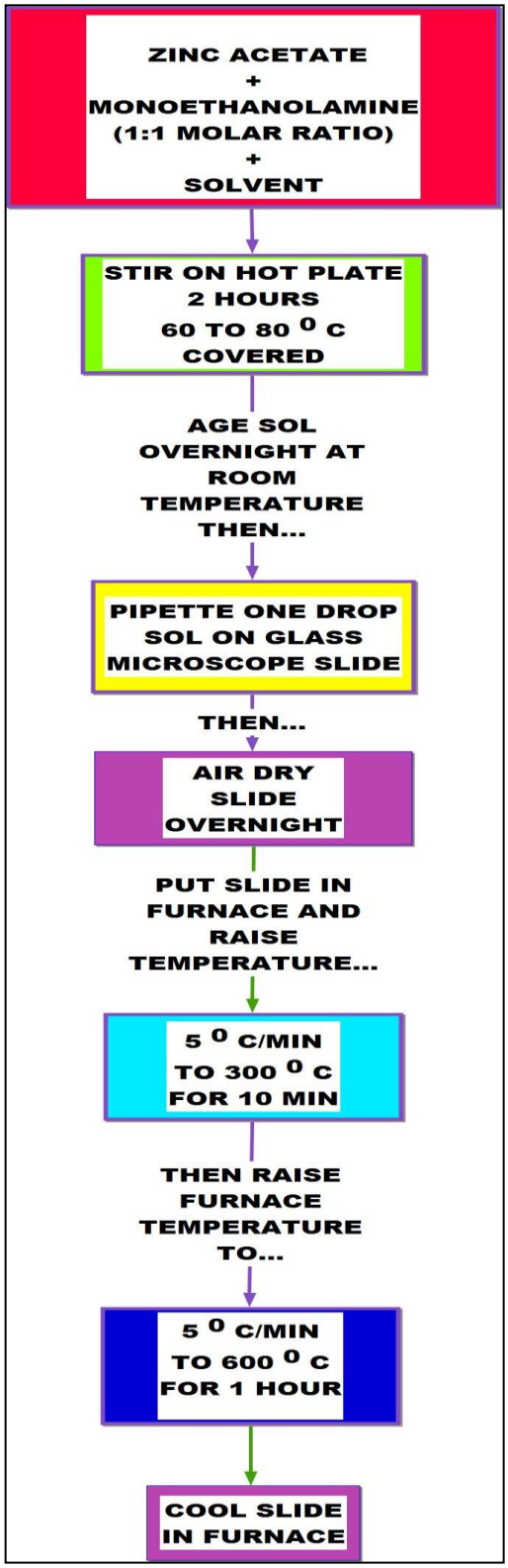


Figure 10: Process Flow Chart for ZnO Sol-Gel Films

**Section II: Evaluation of Key Factors Controlling Organic Based ZnO Sol-Gel**

To evaluate the solvent variable further, sol-gels were synthesized in the same way as described in Section I but the variables that seemed critical to good film formation were expanded as follows:

1. **Effect of solvent:** Three organic solvents were used: Methanol (BDH, 99.8%), IPA and MOE (both same as Section I). The series of solvents were chosen based on being frequently reported in the literature to produce good Zinc Oxide thin films. Also they represent a nice range of boiling point and hydrophobicity behavior as can be seen in Table 12.
2. **Effect of Zinc Acetate Concentration:** 0.5 M and 1.3 M zinc acetate sols were made in each of the solvents mentioned above to test the impact of concentration on the quality of the films produced.
3. **Effect of Film Formation Technique:** To better understand the impact of the process used to make the film on the quality of film produced, two approaches were used as follows:
    - Self-spreading a droplet on a glass microscope slide and letting the film dry horizontally before heat treatment i.e., the same procedure as described in the last section.
    - Dip coating a glass slide into the hot solution and letting the film air dry vertically before heat treatment.
4. **Effect of pH modifier**: Two pH modifiers, MEA and Ammonium Hydroxide (EMD, ACS grade) were evaluated to better understand the role of the pH vs. any stabilizing property might be attributed to MEA.

The specific process conditions used are depicted in Figure 10 and were described in the previous section. The findings from this series of experiments are outlined below.

**Effect of Solvent:** Clear, homogeneous sols were made with all three solvents at both levels of zinc acetate dihydrate as can be seen in Figure 11.

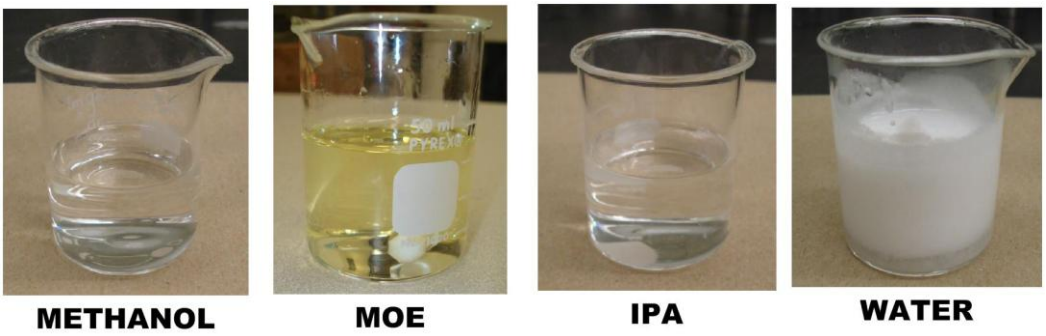


Figure 11: Pictures of Organic Based Sol vs. Water as a Solvent

As in Section I, the resulting MOE films were slightly more transparent to the eye than the IPA films as can be seen in Figure 12. The MOE films were also slightly more transparent then the Methanol films. One hypothesis for why the MOE sols form more transparent films was suggested in literature (ref 10) as a result of MOE's higher boiling point (see Table 12). This was thought to help by allowing the solvent stay in the gel matrix longer during the formation of the crystallography. The boiling point hypothesis will be tested in the next section by evaluating sol-gel's made with an organic solvent with similar boiling point to MOE i.e., n-Butanol.

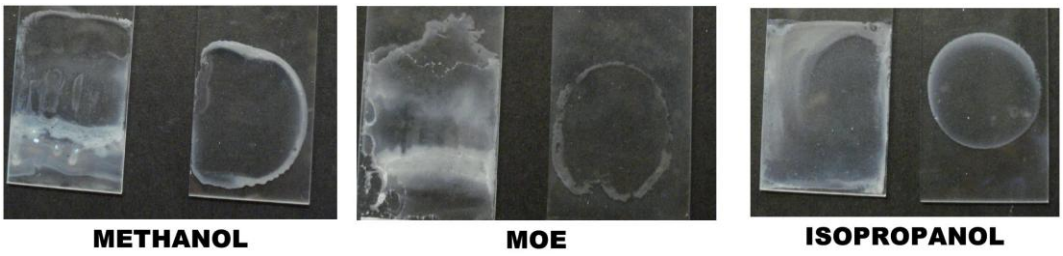


Figure 12: Photos of Zinc Oxide Films for 0.5 M Zinc Acetate Sols

(Different organic solvents (dip coated on left, droplet on right)

**Effect of Zinc Acetate Concentration**: The films made with higher concentrations of zinc acetate (1.3 M) do not have the same level of visual transparency that is seen with 0.5 M Zinc Acetate solutions (see Figure 13). This is consistent with results seen in Reference 1. In that study, 1.3 M zinc acetate showed decreased c-axis orientation resulting in lower optical transmittance due to an increase in light dispersion from grain boundaries.

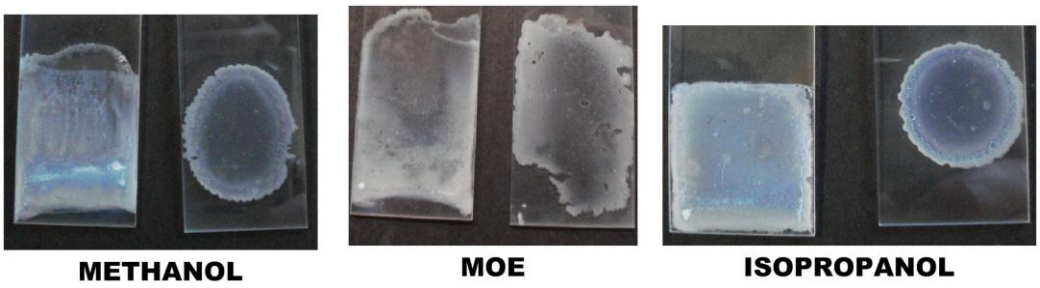


Figure 13: Photos of Zinc Oxide Films for 1.3 M Zinc Acetate Sols

[Different organic solvents (dip coated on left, droplet on right)]

**Effect of Film formation technique:** The technique used to make the films had a dramatic impact on the quality of the film made. The droplet approach produced more consistent and visually transparent films than those made by dip coating - as can be seen in Figure 12 and Figure 13.

**Effect of pH modifier:** The resulting films made with Monoethanolamine (MEA) and Ammonium Hydroxide were about equal for visual transparency (see Figure 14). This suggests that the role of MEA is primarily as a pH modifier as suggested in Reference 5 and 10 and that it is not essential to the cross linking structure as suggested in Reference 9.

**Water as a solvent:** Water was investigated at as a possible solvent for these particular process parameters. The resulting solution was an extremely viscous, thixotropic colloidal suspension as compared to the clear; almost water thin sols that were produced with the organic solvents (see Figure 15). The films made with the water sol were not good. They were full of defects and had very poor crystallography (see Figure 15). A different approach will be needed to make water work as a solvent. This will be the topic of the next chapter, discussed in great detail in Chapter 4.

**Sol-gel stability:** All the solutions were clear and homogeneous when initially made. After one month, all show signs of degradation except for the 0.5 M and 1.3 M zinc acetate solutions made with MOE. The low concentration (0.5 M) Methanol and Isopropanol formed a film on the surface of the storage container. This further confirms what is being seen in film formation i.e. that the MOE sol is more robust for making thin films. It also suggests a potentially novel way of forming films using a 'self assembly' mechanism with the Methanol and Isopropanol. This will be evaluated further in the next section.

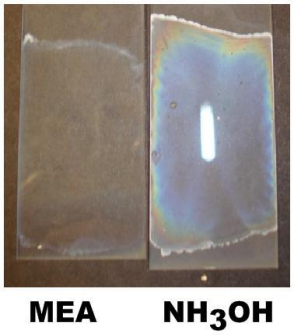


Figure 14: pH Modifier

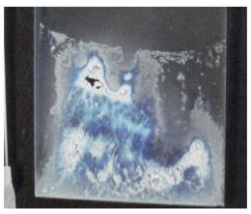

Figure 15: Film from Water Based ZnO Sol

**Section III: Series to Duplicate and Expand Organic Based ZnO Sol-Gel Series**

Compared to the other organic solvents, i.e., IPA and Methanol, MOE is showing better film formation based on visual inspection. Literature references suggest MOE is a good solvent for ZnO sol-gel because of its higher boiling point. 1-Butanol was evaluated to test this hypothesis since it has roughly the same boiling point as MOE (see Table 12). Ethanol was also added to the solvent series so that there would be a complete hydrocarbon series from Methanol to 1-Butanol (also referred to as n-Butanol).

To make the sols, the same process conditions were used as described in Figure 10. A 0.5 molar solution of Zinc Acetate Dihydrate (Alfa Aesar, 98%-101%) was made in 30 ml of solvent using Methanol (BDH, 99.8%), Ethanol (Pharmco-AAPER, 200 proof, USP grade), IPA (Sigma Aldrich , USP grade ), n-Butanol (Sigma Aldrich, 99.4%), and MOE (Sigma Aldrich, 99% or greater, reagent plus grade). In all solutions MEA (Sigma Aldrich, 99% or greater) was added in a 1:1 molar ratio to the Zinc Acetate Dihydrate.

The ingredients were weighed carefully and then added to a glass beaker that had been cleaned with hot soapy water, then distilled water, then acetone and finally with the solvent that was to be used to make the sol. The solution was stirred using a magnetic stirrer on a hot plate kept at 60 - 80$^0$C for 2 hours. Using these conditions, clear, homogeneous sols were made with all solvents. The MOE sol had a bright yellow color whereas all the other sols were colorless. All the sols were water thin.

Films were made on microscope slides (Pearl, precleaned, 1” by 3”) that had been cleaned in boiling distilled water and then rinsed in acetone. A pipette was used to place one drop of each sol near the end of a cleaned microscope slide. The MOE and n-Butanol sols were found to ‘wick’ over a larger area than the other solvents. For an accurate comparison of the optical properties, the size of the film made from a sol droplet needed to be roughly equal. To accomplish this, the droplet of each sol was spread over the glass slide using the end of a pipette that had been ‘wetted’ with the sol. This resulted in films that covered approximately the same amount of area i.e., about two thirds of the microscope slide.

The films were allowed to dry in air over night. Then these films were thermally treated with an initial drying at 300$^0$C for ten minutes followed by an annealing treatment at

$600^0$C for 1 hour. The rate of heating the furnace was 5 $^0$ C/min. The films were allowed to cool in the furnace. Visual inspection indicated that the clarity of the film appeared to be directly related – at least in part – to the boiling point of the solvent. Higher boiling point solvents resulted in films with better visual clarity. This series was duplicated and confirmed the above findings.

To summarize the findings, films made with a droplet of sol on a glass slide were visually better when made with MOE. This could be due to boiling point or the unique chemistry of MOE vs. the series of organic alcohols evaluated. Further work is needed to determine which mechanism is controlling the final film properties. This will be explored further in Chapter 5.

**Section IV: Film Synthesis via Spontaneous 'Self Assembly' in Organic ZnO Sol-Gel**

Sols made with 0.5 M Zinc Acetate Dihydrate in Methanol and IPA were observed several months later to be developing a film on the surface of the vials they were being stored in as opposed to precipitating as particles to the bottom of the vial. This suggested a novel film mechanism might be in play. Specifically, without any evaporation of solvent, films were spontaneously forming and adhering to surfaces. The mechanism by which these films were forming is being referred to in this report as a 'self-assembly' mechanism. The so called 'self-assembly' mechanism, as far as this author is aware, is a unique process for developing zinc oxide thin films via sol-gel. This fabrication process has not been employed or noted in any of the published zinc oxide sol-gel literature.

Whereas the droplet of sol described previously was placed on a substrate and allowed to spread out by capillary action to form a film, the 'self-assembly' mechanism does not appear to require evaporation or capillary action. The mechanism hypothesized for the films being formed by this 'self-assembly' mechanism is believed to be a slower version of the sol-gel mechanism but is initiated by the random nucleation of 'seed crystals' of the 'gel' nanoclusters on surfaces. This initial random nucleation is followed by ordered growth that results in the characteristic sol-gel 'skeleton' of loosely connected ZnO nanoclusters surrounded by sol. The solvent/organic components are normally removed via a drying and annealing step which further condenses the solid 'skeleton' into a good film. But in the 'self-assembly' films the condensation is partially occurring without heat treatment. The spontaneity of this synthesis process has the potential to be a cost effective way to make Zinc Oxide films.

To confirm this, a Methanol sol similar to the one showing 'self-assembly' was made and placed in glass Petri dishes with glass covers. Glass microscope slides were placed in the Petri dishes to 'collect' any film that might form but they were placed horizontally. Samples were drawn once each day. In just 3 days, despite being in covered, not only were films forming but the sol was forming a gel that was much thicker than the initial sol in viscosity. The glass slides that were in the Petri dishes had a very thick film on them that could be dried

and annealed into a film. From this it appeared that the 'self-assembly' mechanism could be a novel way to make Zinc Oxide thin films. However, these films were extremely rough and so the 'self-assembly' fabrication process was modified as described next.

A second sol was made but instead of Methanol, IPA was used as the solvent to slow the rate of 'self-assembly' film formation. The sol was made with the same concentrations and process conditions that were used in the previous labs. As mentioned before, the basic process steps are outlined in Figure 10. A 0.5 molar solution of Zinc Acetate Dihydrate (Alfa Aesar, 98%-101%) was made in 100 ml of IPA (Sigma Aldrich, USP grade). MEA (Sigma Aldrich, 99% or greater) was added in a 1:1 molar ratio to the Zinc Acetate Dihydrate. The ingredients were weighed carefully and then added to a glass beaker that had been cleaned with hot soapy water, then distilled water, then acetone and finally with IPA. The solution was stirred using a magnetic stirrer on a hot plate and kept at 60 - 800C for 2 hours. Using these conditions, a clear, homogeneous sol was made.

Films were made on microscope slides (Pearl, precleaned, 1" by 3") that had been cleaned in boiling distilled water and then rinsed in acetone. The slides were taped to the sides of a beaker in a vertical position and the IPA sol was placed in the beaker where it covered about two thirds of the microscope slide. After 30 days, a thick, white film had formed on the glass slides. The films were allowed to dry in air overnight. Then they were thermally treated with an initial drying at $300^0$C for ten minutes followed by $500^0$C for 1 hour. The rate of heating the furnace was $5^0$ C/min.

The films were allowed to cool in the furnace. Visual inspection indicated that the film was white and opaque – probably due to the fact that it was quite thick. Nevertheless, the 'self-assembly' method appeared to making Zinc Oxide films in a spontaneous and unique manner. Further study is needed to understand the film crystal character and the mechanism by which this is operating. This will be discussed in Chapter 6.

To summarize, visually clear films which appeared to be defect free were made using organic solvents. The best films in terms of a visual inspection of transparency and uniformity were films formed by placing one drop of sol on a microscope slide. The best sol for making films – again based on visual inspection – were those made with 0.5 M Zinc Acetate Dihydrate

and 0.5 M MEA in the solvent 2-methoxyethanol (MOE). The MEA can also be replaced with ammonium hydroxide since it appears that this material strictly functions as a pH modifier and does not act as a stabilizer in the MOE sol. Films can also be formed by a 'self-assembly' mechanism. The best sol for this are the sols based on IPA and possibly methanol. More research needs to be done to explore this synthesize approach.

# Chapter 4: Fabrication of ZnO Thin Films Using Aqueous Sol-Gel

The objective of this work was to produce Zinc Oxide thin films using a modified sol-gel process i.e. one that was based on water as the solvent. This involved:

1. Identifying the process and formulation parameters required to produce a stable sol-gel.

2. Identifying the process and formulation parameters for fabricating good Zinc Oxide thin films.

## Section I: Identification of Key Variables Controlling Aqueous ZnO Sol-Gel Synthesis

In this section, research focus was on the feasibility of replacing the organic solvents with water since the replacement of organic solvents with water would greatly enhance the economics of processing Zinc Oxide thin films. There were only a few references (Ref 21-25) that used water based sol-gel processes to make Zinc Oxide thin films. None of these reports demonstrated the ability to make good c-oriented, transparent and defect free films. Thus, the ability to make a good Zinc Oxide thin film in an aqueous environment was questionable. Therefore this series of experiments were initiated to determine feasibility of making aqueous based Zinc Oxide thin films and the key variables related to this.

### *Part a: Aqueous ZnO Sol-Gels with pH modifier Citric Acid*

The approach initially taken to making aqueous Zinc Oxide sol-gel was based on Ceria Oxide sol-gel processing in aqueous solutions. This involved the use of Citric Acid as the stabilizing/chelating agent. Process conditions were similar to those describe in the last chapter. Two ratios of Zinc Acetate Dihydrate (Alfa Aesar, 98%-101%) to Citric Acid (Sigma Aldrich, Reagent Grade, 98% or greater) were used. As can be seen in Table 7, both solutions were found to be unstable, precipitating a white solid out of the solution within an hour of mixing at 60 - 80$^0$C. The pH of the solution was 2.

Table 7: Influence of Citric Acid on Aqueous Zinc Acetate Solutions

| Reference | 7-8 | 7-9 |
|---|---|---|
| Zinc Acetate Dihydrate | 1 M | 1 M |
| Citric Acid | 2 M | 3 M |
| Solvent | Distilled Water | Distilled Water |
| Mixing conditions | 1 hour at $80^0$C | 1 hour at $80^0$C |
| Resulting 'solution' | Precipitates | Precipitates |

These experiments suggested that – much like the organic sol-gel's - acidic conditions were **not** feasible for making Zinc Oxide thin films. Given what the literature had reported about higher pH being conducive to the formation of good Zinc Oxide sol-gel processing as well as what was observed in Chapter 3, it was determined to evaluate aqueous Zinc Oxide sol-gel with alkaline pH.

***Part b: Influence of Ammonium Hydroxide on Aqueous ZnO Sol-Gel***

Combinations of Zinc Acetate Dihydrate (Alfa Aesar, 98%-1010%) in distilled water with Ammonium Hydroxide (EMD, ACS grade) were evaluated next. A solution of 0.5 M Zinc Acetate Dihydrate in distilled water was stirred at $50^0$C at which point the Ammonium Hydroxide was added. The solution immediately increased in viscosity, becoming an extremely viscous, unstable colloidal suspension. The mixture was cloudy with evidence of a solid precipitate dispersed in a gel matrix. Even very small amounts of Ammonium Hydroxide resulted in a thixotropic colloidal suspension that was unstable (see Table 8).

Table 8: Influence of Ammonium Hydroxide on Aqueous Zinc Acetate Solutions

| | |
|---|---|
| Reference | 7-24A and 8-5B |
| Zinc Acetate | 0.5 M |
| 28% solution of ammonium hydroxide in water | 1 g of solution |
| Solvent | 40 ml Water |
| Resulting colloidal gel | Cloudy, viscous gel with visible particles of solid suspended, unstable |

***Part c: Influence of Monoethanolamine on Aqueous Zinc Oxide Sol-Gels***

A solution of 0.5 M Zinc Acetate Dihydrate (Alfa Aesar, 98%-101%) in distilled water with Monoethanolamine was made using ratios similar to what is used in organic Zinc Oxide sol-gels. This was to see if the 'stabilizing' role reported in the literature for organic solvent sol-gels would bring about stable aqueous sol. It did not stabilize the sol as can be seen in Table 9. In fact, a result similar to what was seen with Ammonium Hydroxide was observed. The solution formed was a cloudy, viscous, unstable colloidal suspension upon the addition of the Monoethanolamine. The pH of the solution was about 6. The gel separated into two phases after it had cooled. Films made with this sol and the Ammonium Hydroxide sols were unacceptable.

Table 9: Influence of Monoethanolamine on Aqueous Zinc Acetate Solutions

| Reference | 7-24A |
|---|---|
| Zinc Acetate | 0.5 M |
| Monoethanolamine | 0.5 M |
| Solvent | Water |
| Resulting colloidal gel | Cloudy, viscous gel with visible particle suspended, unstable |

***Part d: Influence of Ammonium Hydroxide plus Citric Acid on Aqueous ZnO Sol-Gels***

Finally, combinations of Zinc Acetate Dihydrate in distilled water with both Ammonium Hydroxide and Citric Acid were evaluated. When a one to one molar ratio of Citric Acid to Zinc Acetate Dihydrate was used with enough Ammonium Hydroxide to bring the pH up to about 8, the resulting sol was clear, homogeneous, and water thin (see Table 10).

Table 10: Influence of $NH_3OH$ plus Citric Acid on Aqueous ZnO Sol-Gel

| Reference | 7-14 & 7-24B2 | 8-5A | 8-5B | 10-13 |
|---|---|---|---|---|
| Zinc Acetate | 0.5 M | 0.5 M | 0.5 M | 0.5 M |
| Citric Acid | 0.5 M | 0.15 M | 0.05 M | 0.009 M |
| 28% $NH_4OH$ Solution | 10 g | 3 gram | 1 gram | 0.1 g |
| Solvent | Water | Water | Water | Water |
| Resulting 'sol' | Clear homogeneous water thin solution | Clear homogeneous water thin solution | Visibly thicker and lumpy | Clear homogeneous water thin . |
| | Beads up on substrate then dries to a powder | Beads up on substrate then dries to a powder | Cloudy, lumpy film | Beads up on substrate then dries to a powder |

Reduced levels of Citric Acid were evaluated to determine if a clear sol could be achieved with higher viscosity. At low levels of Citric Acid it was thought a more gel like sol could be achieved since the experiment with no Citric Acid produced a very viscous – though unstable gel. However, when the Citric Acid was reduce to about one third the molarity of Zinc Acetate Dihydrate, the solution was still clear but also still thin.

Films formed with low levels (less than the 0.5 M) of Citric Acid were not good in that they tended to form powder rather than a film. This will be discussed in more detail in the next section on film formation. When the Citric Acid level was reduced even lower (0.05 M), the sol became thicker but also became cloudy with visible lumps. When the Ammonium Hydroxide is reduced in level, the sol clears up and simultaneously gets thinner. However, again, at low levels, poor films result as will be discussed in the next section.

To summarize, the ideal levels for producing a clear and stable water based sol appear to be 0.5 M Zinc Acetate Dihydrate with 0.5 M Citric Acid and a small amount of Ammonium Hydroxide to provide a pH of 6 to 8. This suggests that the Citric Acid is essential to aqueous Zinc Oxide sol-gels as a stabilizing agent. It was hypothesized that the hydroxyl groups on the Citric Acid (see Table 13) chelate the Zinc Hydroxy Acetate nanoclusters, thus helping the cross linked network of microparticles stay in solution long enough for the 'micro skeleton' of solid particles to coalesce. The ‘sol’ of course must still be alkaline to make the hydroxyl groups available- similar to what was seen in the organic based sol-gel work. Although this is a stable sol, it will not form films on glass slides. It could have potential applications for forming nanostructures with templates.

## Section II: Evaluation of Key Variables in Film Formation of Aqueous ZnO Sol-Gels

### *Part a: Initial evaluation of Key Variables in Film Formation of Aqueous ZnO Sol-Gels*

The synthesis of thin films out of an aqueous matrix on a simple glass slide is more challenging than Zinc Oxide sol-gels made with organic solvents. The stable aqueous sol described in the last section i.e., 0.5 Molar Zinc Acetate Dihydrate with 0.5 M Citric Acid and ammonium oxide exhibited the following film formation issues:

- When a drop of the sol is placed on a glass slide it beads up into a droplet. The droplet then dries to a powder rather than a film. In comparison, the organic based sols will form a film when dropped onto a glass substrate.
- Several other substrates were evaluated such as copper, aluminum, nickel alloys and silicon. The aqueous sols bead up on these substrates as well, drying again to a fine power.
- Spin coating the sol results in the liquid simply flying off the substrate as a result of the centrifugal force overcoming the surface energy of the liquid for the glass substrate. In comparison, the organic based sol will form a good, transparent film with spin coating.
- Heating the sol and then applying that to a glass slide and drying the slide in a vertical position does result in a film that is free of defects and is transparent in localized areas. The film is not homogeneously thick however. It is transparent at the 'top' where it is thinner and translucent at the 'bottom' where it is thicker.
- Surface treatment of the glass slide with the organic sol does not improve the ability to make a film via the aqueous sol.
- A more dilute sol and more concentrated sol were made and found to behave similarly as the 0.5 M sol.
- When surfactant (Palmolive dish detergent) is added to the aqueous sol, a film will form on the glass substrate. The sol will spread out on the glass and dry to

a translucent film. Although the film did not have a homogeneous morphology, this was the first evidence that a Zinc Oxide thin film was possible with an aqueous based sol-gel. In addition, this suggested modification of the sol's surface characteristics might be the key to producing acceptable films.

***Part b: Modification of Aqueous ZnO Sol-Gel Formulation to Achieve Film Formation***

The previous research indicated that film formation would be the major challenge for aqueous based Zinc Oxide sol-gels. There were two approaches to addressing this problem: 1. Modify the sol-gel so that is has better surface adhesion to the glass substrate; or 2. Modify the substrate so that it is more compatible with the aqueous sol. The first approach was the focus of this research.

As mentioned earlier, one of the most promising approaches was to modify the aqueous sol (consisting of Zinc Acetate Dihydrate, Citric Acid and Ammonium Hydroxide in water) with wetting agents such as surfactants. Suspension/thickening polymeric compounds were also hypothesized to be viable candidates for aiding aqueous thin film formation.

Therefore a variety of compounds were explored in the aqueous sol's which would test a range of hydrophobicity, electronic charge, and viscosity as follows:

**Wetting Agents:**

- PEG-7 glycerol cocoate: **a nonionic surfactant**.
- Diethanol amine salt of pelargonic acid: a cationic **surfactant.**

**Thickeners/suspension agents:**

- Carbomer: an **anionic synthetic polymer** of acrylic acid.
- PVA (Polyvinyl alcohol): a **nonionic synthetic** polymer.

Anionic surfactants were **not** evaluated because the hydrophilic group usually contains sulfur which had the potential to contaminate the Zinc Oxide films.

After an initial screening, it became obvious that the thickeners showed film formation potential whereas the wetting agents did not. The wetting agents, although helping to prevent the sol from beading on the glass, interfered with the film formation often resulting in powders or puff balls rather than films. In contrast, the polymeric thickening agents produced films that were visually clear but with flaws where the film had been too thick. This suggested further formulation might successfully produce films.

***Part c: Final Evaluation of Aqueous ZnO Sol-Gel Film Formation***

A range of polymeric thickeners were evaluated including PVA, Hydroxyethyl Cellulose (HEC), Xanthan Gum, and Guar Gum. The chemistry of these compounds is shown in Table 11. All of these thickeners formed films.

The best films were those made with a sol that contained only water and Zinc Acetate Dihydrate. In other words, removal of the Citric Acid and pH modifier was necessary to obtain stability in a Zinc Acetate Dihydrate sol using thickening agent. With this modification good films were developed that were **crystal** clear and in fact looked quite different – visually – from the films made with organic solvents. However, the films were not homogeneous in thickness – there was still evidence that the sol was beading up on the glass substrate although less so. It was clear that substantial formulation work would be needed to use water as a solvent that would yield consistent film results.

Nevertheless, water based sols hold the promise of tremendous cost effectiveness as a sol-gel process. In addition the films appeared to form unique ZnO film morphology. This will be discussed more in the next chapter.

Table 11: Polymeric Thickening Agents

| Material | Description | Structure |
|---|---|---|
| Polyvinyl alcohol | A nonionic polymer: prepared by partial or complete hydrolysis of polyvinyl acetate to remove acetate groups. | 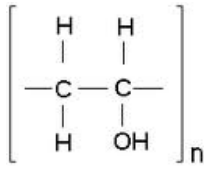 |
| Guar Gum | A cationic polysaccharide a naturally derived, quaternary, high-molecular weight polysaccharide. | 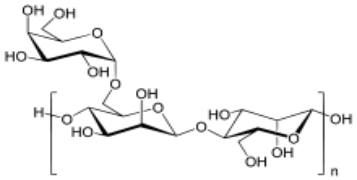 |
| Xanthan Gum | An anionic polysaccharide composed of pure natural polysaccharides (sugars) constituted of glucose, mannose and glucuronic acid. | 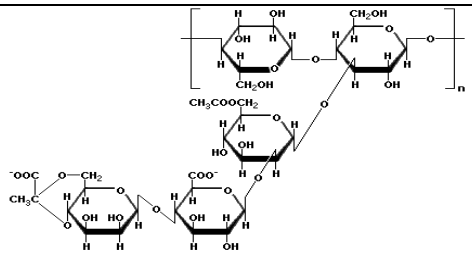 |
| Hydroxyethyl cellulose | A nonionic polysaccharide derived from cellulose. | 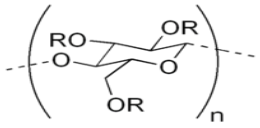 R = H or $CH_2CH_2OH$ |
| Carbomer | An anionic thickener than is a polymer of polyvinyl carboxy groups. | 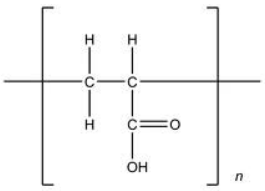 Acrylic acid monomer unit in carbomer polymers. |

# Chapter 5: Optical Performance of ZnO Thin Film via UV-Vis Spectrophotometry

## Section I: Background on UV-Vis Spectrophotometry

For applications in renewable energy devices, the Zinc Oxide films must have good transparency to visible light. Ultraviolet-Visible (UV-Vis) Spectrophotometry is a good method for characterizing film transparency. Also, because this method looks at electronic transitions (Ref 45.), the analysis can be used to analyze the band gap of a material by using Equation 7:

$$E = hc/\lambda \qquad (7)$$

In this equation, 'E' is energy, 'h' is Planck's constant with a value of $4.13 \times 10^{-15}$ eV sec, 'c' is the speed of light with a constant value of $3 \times 10^{8}$ m/s and finally 'λ' is the wavelength taken from the absorbance peak on the UV-Vis spectra.

Figure 16: UV-VIS Spectrophotometry

Identifying the band gap absorption peak from the UV-Vis spectra helps to characterize a material. Zinc Oxide is known to have a band gap of approximately 3.3 eV (ref 64). This results in an absorption peak at approximately 3.76 E -7 meters, or 376 nm, in the UV-Vis spectra as determined by Equation 8. This also means that ZnO films should be transparent to light that is roughly 380 nm or higher.

$$4.13 \times 10^{-15} eV \sec \times 3 \times 10^{8} \frac{m}{s} \div 3.3\ eV = 3.76 \times 10^{-7}\ m \qquad (8)$$

The model of the UV-VIS spectrophotometer used in this research was a Cary Varian 50 BIO UV Visible Spectrophotometer. The X-mode, representing the range of light wavelength used for detection of light transmission, was set at 200 to 800 nanometers. A dual light beam was used to provide full coverage of the visible and UV wavelengths. Baseline measurements were taken with a blank microscope slide (Pearl, precleaned, 1" by 3") since this was the substrate used in film formation. UV-Vis data on films were compared to the absorption profile of a blank microscope slide to determine the optical transmittance and maximum absorbance of the film.

The Cary Varian UV-Vis Spectrophotometer reports results in terms of the light absorbance. The data generated represents the ratio of the light that passes through the sample to a full beam with no interference except for the blank microscope slide. The equation that describes this is as follows:

$$\text{Absorbance (A)} = \log_{10}(P_s/P_t) \qquad (9)$$

In Equation 9, '$P_s$' is the light absorbed and '$P_t$' is the total light with no absorption. To convert this to the percent of light that is transmitted through the sample, the following Equation was used:

$$\% \text{ Transmission} = 10^{(2-A)} \qquad (10)$$

**Section II: Optical Properties of ZnO Films vs. Low Temperature Thermal Treatments**

Optical transmittance of Zinc Oxide thin films was studied as the films progressed through the low temperature thermal treatments which represented 'drying' phases of the sol-gel process described in Chapter 2, i.e., temperatures from 100 to 250$^0$C. A 0.5 M MOE sol was used as described in Chapter 3. Prior to making the films, the substrate for the films, i.e, 'Pearl precleaned' microscope slides, was cleaned in boiling water and then rinsed in acetone and allowed to air dry. Films were made by placing one drop of sol near the bottom of a microscope slide. The films were allowed to dry in air overnight and then were placed in a furnace.

The thermal drying treatments were done in a series of incremental steps of 50 $^0$C which included temperatures of 100$^0$C, 150$^0$C, 200$^0$C and 250$^0$C. The furnace was kept at each incremental temperature for ten minutes. The rate of heating the furnace was 5 degrees Celsius per minute up to one of the temperatures listed above. The films were not cooled in the oven but instead were removed immediately after the thermal treatment was completed. Also included in this series was the sol without any thermal treatment. These samples were tested for optical transmittance using UV-Vis Spectrophotometry. The results are shown in Figure 17.

The UV-Vis spectra for the sol and the film dried at 100$^0$ C do not show an absorption peak at 380 nm, indicating that no Zinc Oxide is present in these samples. In contrast, films thermally treated at 150$^0$C and above do show an absorption peak at 380 nm, indicating that Zinc Oxide is present. Also, the optical transparency improves as temperatures increases from 150 $^0$C to 250 $^0$C, suggesting increased development of ZnO nanocrystals.

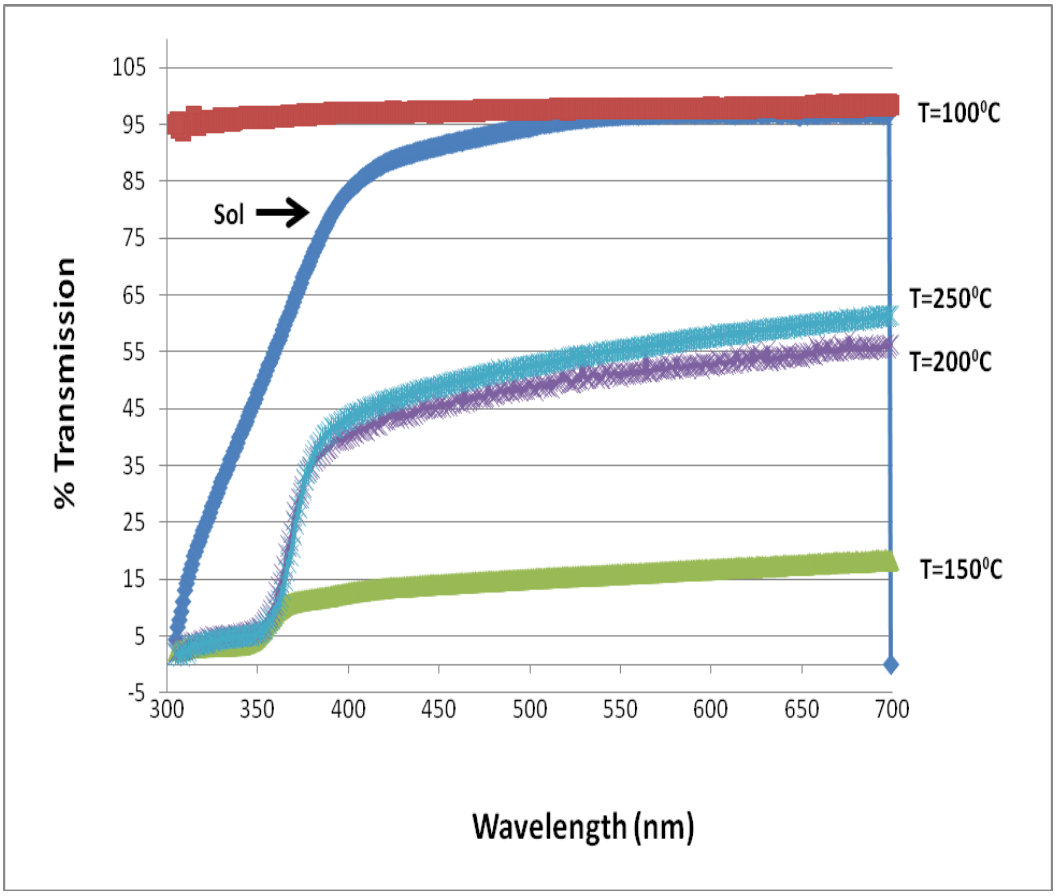


Figure 17: Low Drying Temperatures vs. Optical Properties

**Section III: Optical Properties of ZnO Films vs. High Temperature Thermal Treatments**

Building on the above film formation findings, a second study to evaluate the optical transmittance of Zinc Oxide thin films as they progress through the annealing cycles described in Chapter 2 (i.e., temperatures above $300^0$C) was done. Films were again prepared using the MOE sol with 0.50 M Zinc Acetate Dihydrate. Like the previous study, films were made on glass microscope slide that had been cleaned in boiling water, rinsed in acetone and air dried. The films were made by placing a drop of sol near the end of the microscope slide. Following this the films were allowed to dry in air overnight and then thermally treated for 1 hour at temperatures ranging from $125^0$C to the high annealing temperatures of $400^0$C, $500^0$C, and $600^0$C. The rate of heating the oven was 5 degrees Celsius per minute up to one of the temperatures above. The films were allowed to cool in the furnace. The UV-Vis spectra for the films are shown in Figure 18.

The $400^0$C and $500^0$C films were about equal with an optical transmittance of 90% in the visible range. The films exhibited the characteristic Zinc Oxide 380 nm absorption peak. Recall that these films were estimated earlier to be approximately 400 nm thick. Thus the optical transparency appears to be on par with that which has been reported in literature (ref 1-15) for films with 200 to 400 nm thicknesses. Also of note is that these films were made with a one-step thermal treatment as opposed to the earlier two-step drying then annealing process. This suggests that this process leads to acceptable films without the initial drying step thus greatly simplifying the thermal treatment procedure. Finally, one last note is that obtaining exact measurements of the film thickness made by the droplet approach is important to confirm optical properties relative to other research. This will be discussed in Chapter 7.

The $600^0$C film shows a drop in optical transmittance. This could be due to strain on the crystal structure due to a mismatch in thermal expansion coefficient between the Zinc Oxide crystal and the glass substrate, particularly since $600^0$C is approaching the 'softening

point' for glass. The result of the strain could lead to defects in the Zinc Oxide film that would reduce transparency.

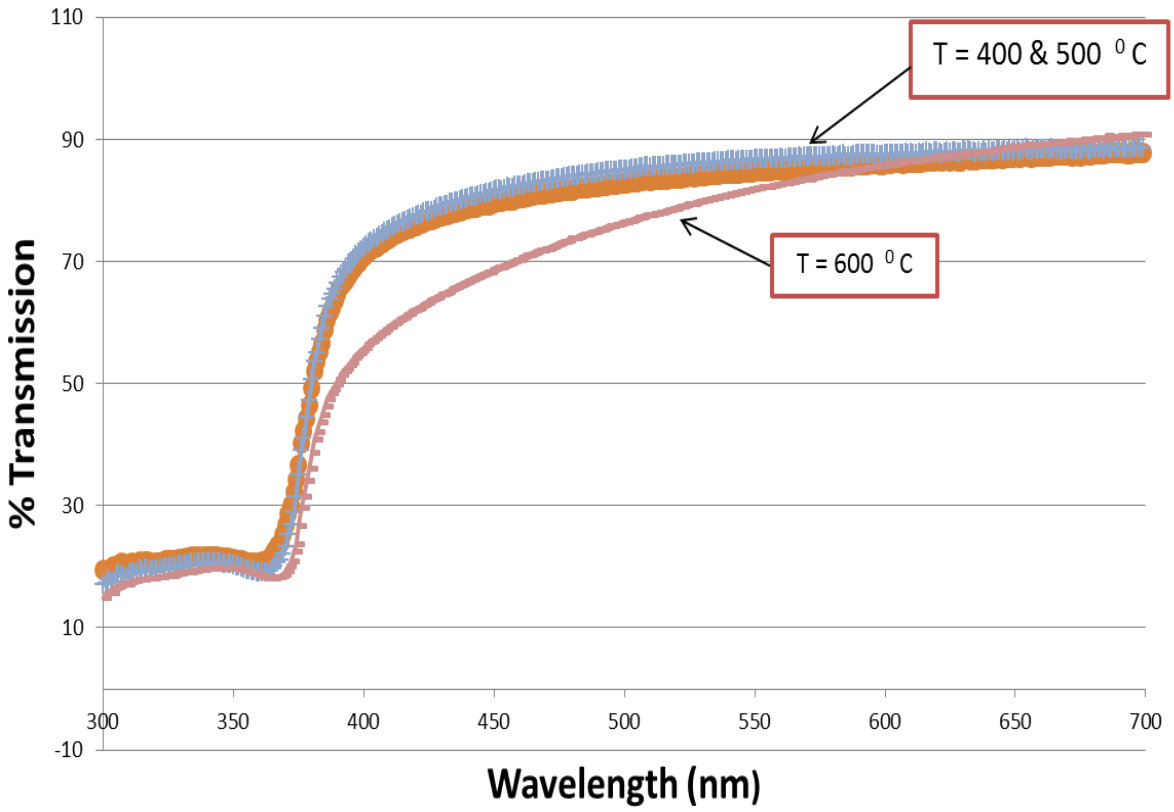


Figure 18: Annealing Temperature vs. Optical Properties

The UV-Vis spectra show interesting changes in the Zinc Oxide crystals as the temperature increases from the low temperature thermal treatments which dry the sol-gel to the high temperature thermal treatments which anneal the Zinc Oxide film. The spectra have been offset to allow clear visualization of the absorption peaks. The development of a sharper, more defined Zinc Oxide absorption peak is evident as the temperature of the thermal treatment increases from 125$^0$C to 600$^0$C (see Figure 19).

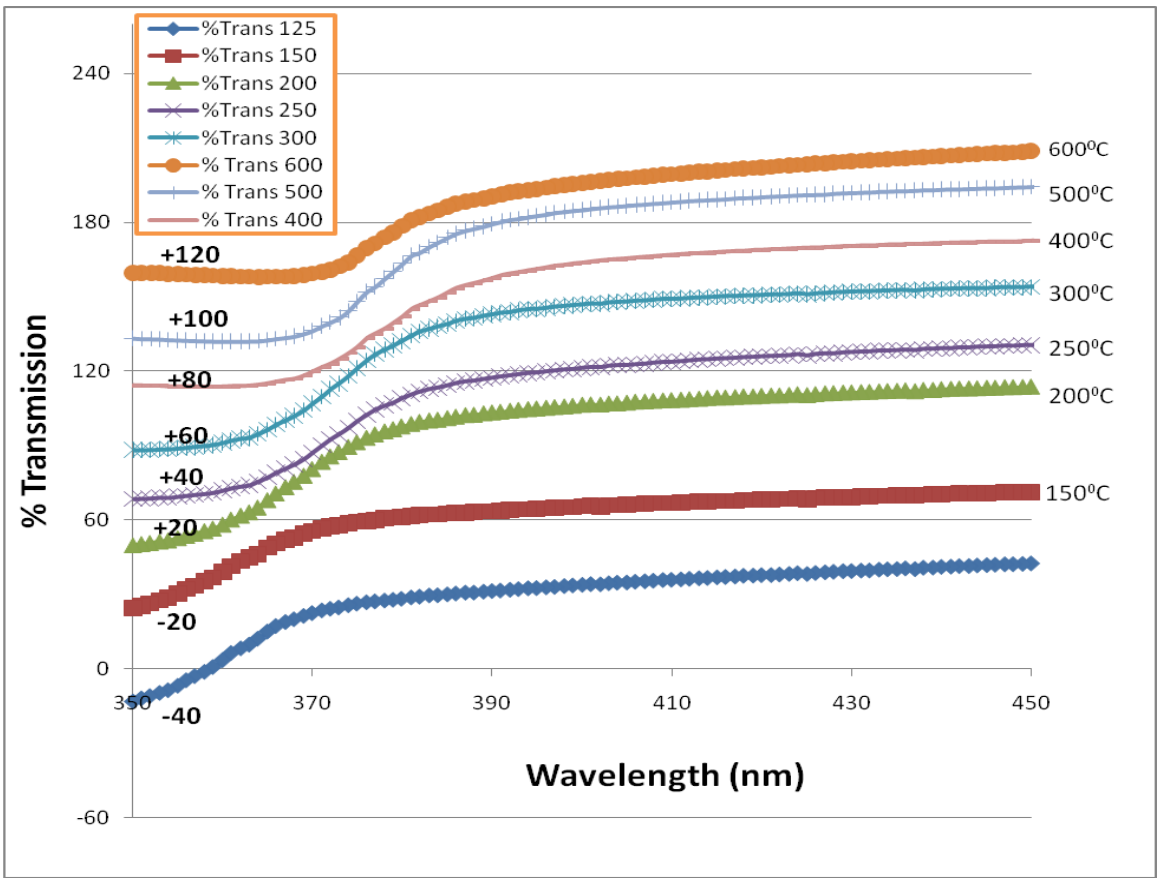


Figure 19: Band Gap Absorption Profile vs. Thermal Treatment

It is also interesting to observe the 'blue shift' in the band gap wavelength in films thermally treated at low temperatures in comparison with those treated at the high annealing temperatures. The absorption peak was slightly shifted to lower wavelengths relative to Zinc Oxide's characteristic absorption peak of 380 nm. This is shown in Figure 20. The 'blue shift' is characteristic of Zinc Oxide nanoparticles and is therefore indirect evidence that the grain size at the low temperature is small enough to experience quantized effects (ref 64). As the temperature rises to $300^0$C or higher, the absorption band is close to the characteristic band for Zinc Oxide of 380 nm.

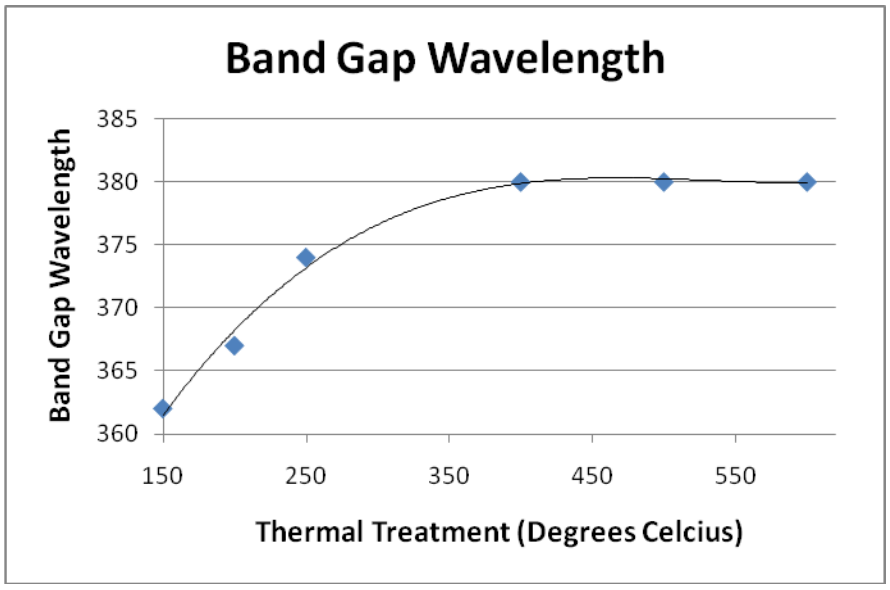


Figure 20: Observed Blue Shift at Low Thermal Treatments

**Section IV: Optical Properties of ZnO Thins Films vs. Organic Solvent**

As mentioned earlier, the solvents reported for making Zinc Oxide thin film sol-gel have included MOE, n-Butanol, IPA, Ethanol and Methanol. Because solvent was found to be a key variable with regard to stability as well as visual clarity of the samples, UV-VIS testing was done on films made from each solvent in an attempt to quantify the differences that were being observed visually.

A 0.5 molar Zinc Acetate Dihydrate sol was made with each solvent as described in Chapter 3. However, when the drop was placed at the end of a glass microscope slide, the sol was spread over a constant area of the slide using the end of a pipette which had been wetted in the sol. This was to help control the film thickness by keeping the area of the slide covered by the sol constant.

The modification in film formation procedure was necessary to obtain accurate UV-Vis comparisons between solvents. Without this adaptation the lower boiling point solvents would have formed smaller and thus thicker films. As a result of this, a direct comparison between solvents would have been inaccurate. The modified film formation method (i.e. manually spreading the films out to cover an equal area on the microscope slide that was roughly equivalent) eliminated the potential differences in film thickness. This adaptation allowed making direct comparisons between solvents reasonable. To ensure that this was in fact the case, the experiment was duplicated and the results were shown to be reproducible.

The UV-Vis spectra for the various solvents are shown in Figure 21. The boiling point of the solvent was found to correlate closely to the optical transparency of the films (see Table 12). This is consistent with the hypothesis that a higher boiling point may lead to more optically transparent films as a result of this slowing down the conversion of the original Zinc Acetate solution to the gel phase. Slower rates would facilitate the development of a Wurtzite crystal structure with a c-axis orientation, that is, with the c-axis is parallel to the normal of the substrate.

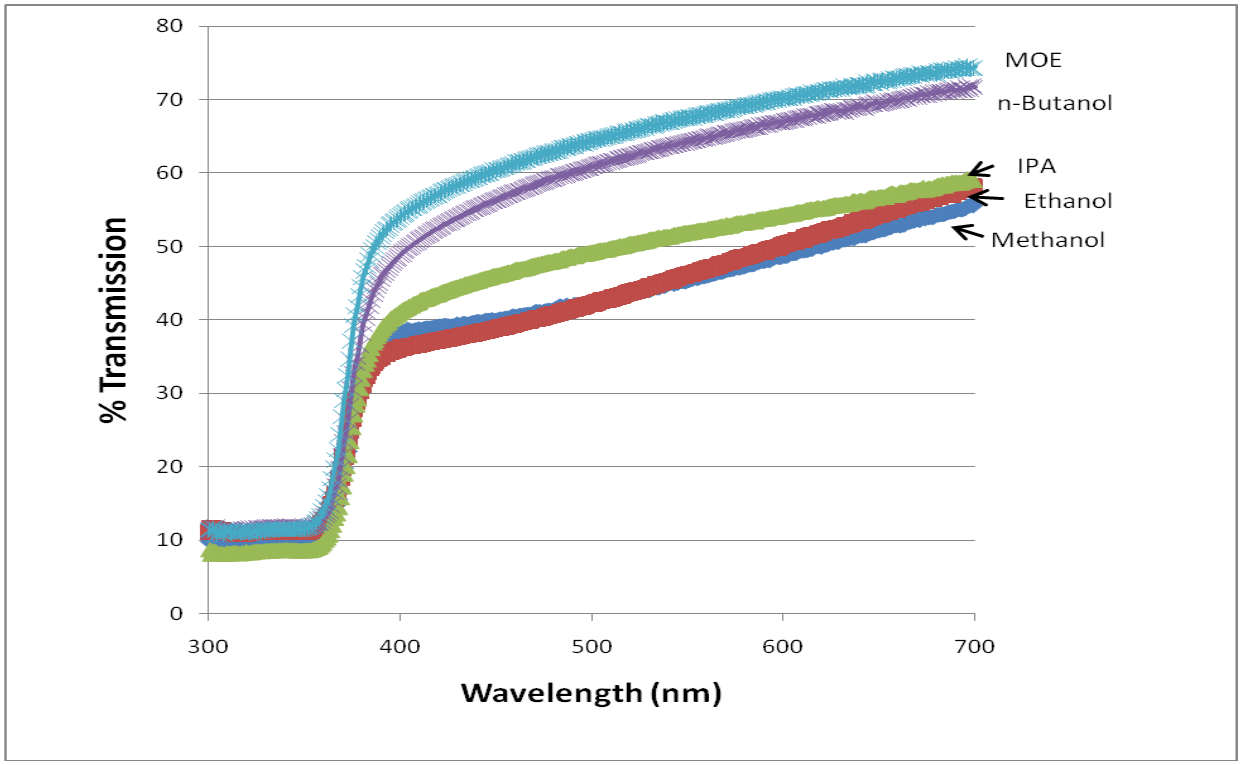


Figure 21: Optical Properties of ZnO Thin Films from Different Organic Solvents

Table 12: Solvent Boiling Point Data

| Material | Boiling Point ($^0$C) |
|---|---|
| MOE: 2 Methoxyethanol | 125 |
| n-Butanol | 118 |
| IPA: Isopropanol | 82 |
| Ethanol | 78 |
| Methanol | 65 |

**Section V: Optical Properties vs. ZnO Aqueous Sol-Gel**

The aqueous based sol-gel films exhibited good transparency when films were formed (see Figure 22). Visually, the films were crystal clear and had a distinctly different appearance from the films fabricated from organically-based sol-gel. Atomic force microscopy shows very dense particle distribution in the films made from aqueous based sol-gels (see Figure 23). However, consistent film formation continued to be an issue throughout this research. Additional study is needed to make any solid conclusions beyond saying that there is potential in this area to make good ZnO films.

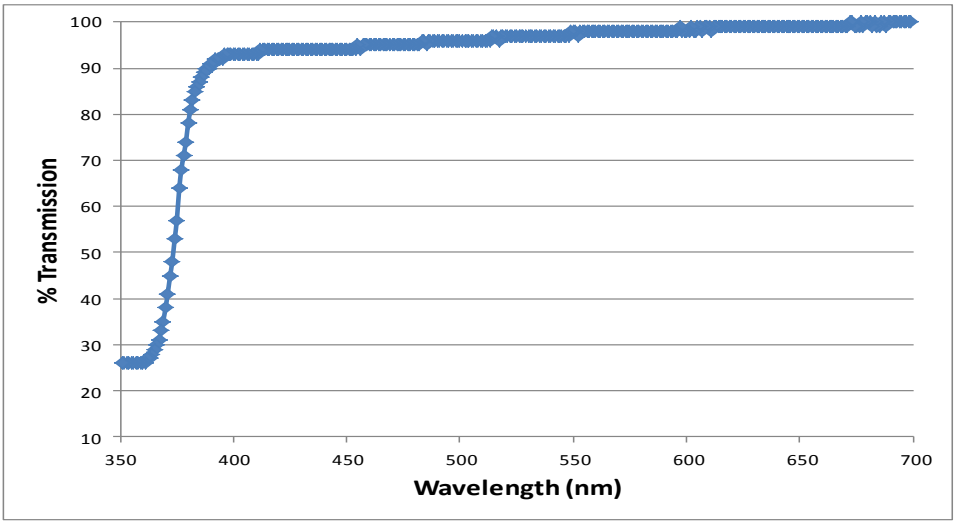


Figure 22: Optical Properties vs. Aqueous Sol-Gel with PVA

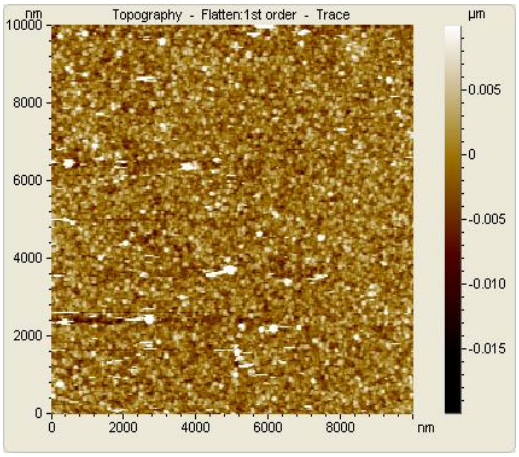


Figure 23: Atomic Force Microscopy of Aqueous Sol-Gel Film with PVA

To summarize the findings from the UV-Vis Spectroscopy work:

The thermal treatment – as expected – is crucial to the development of the final thin film. Zinc Oxide crystals begin to appear between $100^0$C to $150^0$C in a MOE based sol. The optical transparency then continues to increase through the drying phases reaching a maximum transparency of 45 to 65%. Up to that point, the crystal particles experience a 'blue shift' in the absorption band, likely due to quantized effects that may result from particles being in the 5 to 10 nanometer range. Annealing films for one hour at $400^0$C and $500^0$C further improves transparency of the film with optical transmittance as high as 90% in the visible range. Higher temperatures of $600^0$C results in decreased optical transmittance, likely as a result of the thermal expansion coefficient difference between the ZnO Wurtzite and the glass substrate. Another factor could be that the glass is approaching its softening point which could further exacerbate issues with the film integrity.

The solvent also has an important impact on the final film's optical properties. It appears that the boiling point of the solvent is strongly correlated to the final optical transparency with higher boiling point solvents, such as n-Butanol and MOE, bringing about better optical properties. The fact that the MOE is a different color (bright yellow) than all the other sols (which are colorless) combined with the fact that this sol is extremely stable suggests that there may be a chemical mechanism that is involved in addition to the boiling point mechanism. This will be explored in the Chapter 6.

Water has potential to be an excellent Zinc Oxide sol-gel solvent both in terms of film quality and cost effectiveness. However, additional research is needed to obtain consistent film formation and to fully understand the film morphology of this promising lead.

# Chapter 6: Mechanistic Understanding via Raman Spectroscopy

## Section I: Raman Spectroscopy Methodology

Raman spectroscopy is a noninvasive, powerful analytical technique that provides in-depth information about the composition of a material. The analysis relies on the so called 'Raman Effect' which occurs when a photon of light experiences an inelastic collision with the material under investigation. The inelastic collision can result in the photon either increasing or decreasing in energy. The 'Raman Effect' is directly related to the vibrational modes characteristic of the material being analyzed. Each material has its own characteristic energy levels that provide detailed information of the material properties. "Raman scattering is a very sensitive technique to probe local atomic environments. Indeed the properties of the vibrational modes are basically determined by the mass, bond type and symmetry of the constituting atoms in the elemental unit of the gas or liquid (molecule) or solid (primitive cell). In this fashion, the surroundings of a particular atom have a strong influence on its dynamics; therefore any physical factor affecting short range order, such as defects or impurities have a direct impact on the atom vibrational properties. Such modifications in the vibrational characteristics are readily noticeable in the Raman spectrum features." (Ref 40) A diagram of the method is shown in Figure 24.

Figure 24: Raman Spectroscopy

(Pictured is Adam Stahler)

The Raman analyses were performed using a LabRamHR 800 system (Horiba Jobin Yvon Inc.) equipped with 600 and 1800 grooves/mm holographic gratings. The 600 grooves/mm grating system was used for collecting all Raman spectra except for the ones of the ZnO films. The spectral resolution was 1.12227 $cm^{-1}$ and 0.28266 $cm^{-1}$ for the 600 and 1,800 grooves/mm grating systems, respectively. The 633 nm output of a He-Ne laser was used as an excitation line. The laser power output was 22.5 mW with a power at the sample of 15 mW when taken without filters. Filters were used only on the sol spectra which reduced the power to 3.75 mW. The laser beam spot had a diameter of about 1 µm and was focused on the samples with the help of a high resolution confocal Raman microscope (high stability BX41) and long working distance Olympus objectives (50x for liquids and 100x for solids). The confocal hole was set at 300 µm and the backscattered Raman signal was recorded using an open electrode thermo-electric cooled CCD detector (1024x526 pixels). The Raman data were then analyzed and processed using the LabSpec 5 and Origin 8 software.

Literature reports regarding Raman analysis on Zinc Oxide thin films made via sol-gel are very limited. In fact, only one report was identified (ref 42). The conclusion from this study was as follows: "The ZnO films Raman investigation reveals the presence of stresses within the structure of the film. The behavior of the peak *E2* confirms that the microcrystalline grains forming films grow when the deposit solution is aged at $60^0$C. SEM confirms this result. The Raman investigation of the deposit solution proves that Zn – O bonds play probably the role of the initiation of the crystallization during the treatment of the films." The change in the E2 phonon mentioned in this quote is the characteristic Zinc Oxide Wurtzite vibrational mode of 438 $cm^{-1}$. An increase in the E2 phonon vibrational mode was ascribed to compressive stress in the film whereas a decrease in this mode was ascribed to tensile stress. This stress was attributed to a mismatch in thermal expansion coefficients between the glass substrate and zinc oxide films.

The spectra of the films from this literature report are shown in Figure 25. The study reports that the ZnO transversal modes at 380 and 408 $cm^{-1}$ do not appear in the Raman spectra of the films. The second order modes at 331, 531 and 1150 $cm^{-1}$ also disappear on films spectra. The lack of peaks at the transversal and the second order modes is reported to reflect a decrease of the crystallization quality compared to ZnO bulk.

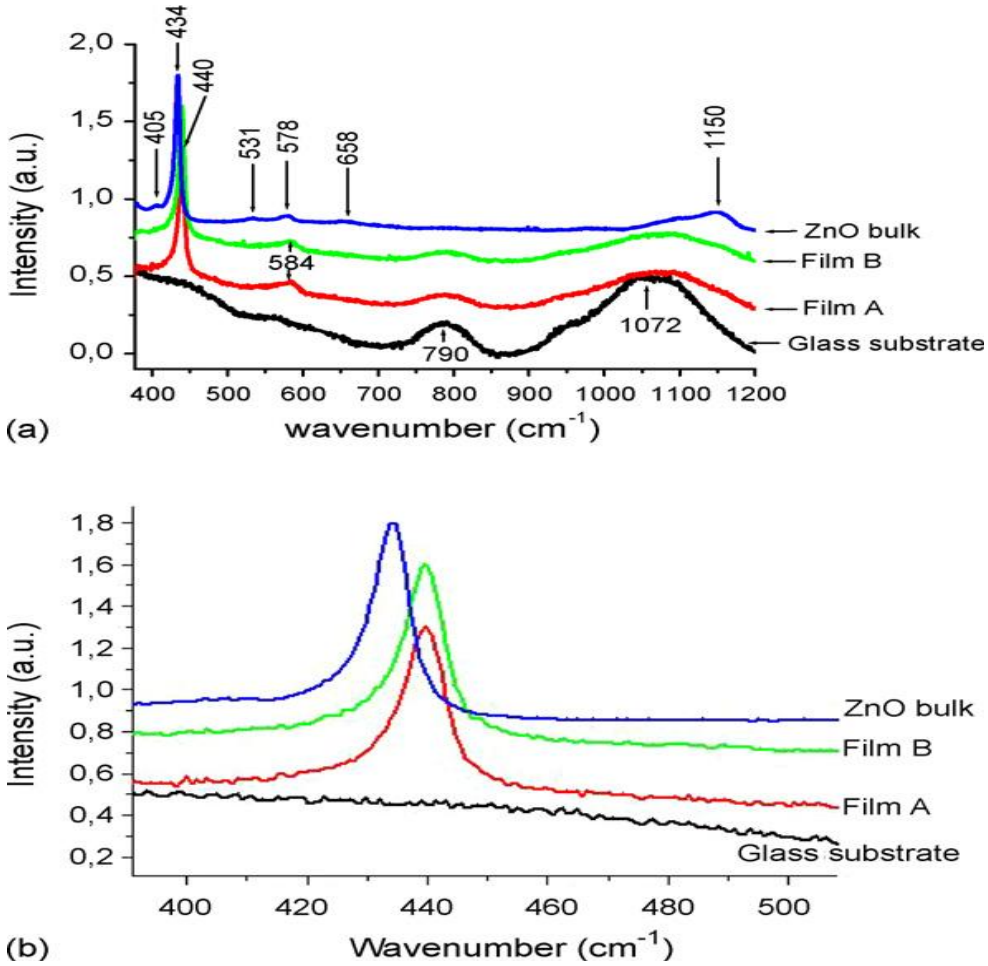


Figure 25: Raman spectra from Reference 42 of ZnO Thin Films Made by Sol-Gel Fabrication

**Section II: Mechanistic Understanding of ZnO Sol-Gel Process**

-Reproducibility and aging affects: To determine the reproducibility of the process being used to make MOE sols in this research, Raman spectra were taken of two different MOE sols that had been produced on two different dates and analyzed on the same date and time. Acquisition time for both spectra was 30 seconds and each spectrum was averaged over three cycles. The results are shown in Figure 26.

The Raman spectra look almost identical, indicating good reproducibility in making the sol. Importantly this also addresses the issue as to whether aging the sol is important to the formation of the zinc/hydroxy cross linking that allows the sol to condense to a continuous film rather than nanoparticles. Two sols with the same formulation had been made approximately 6 weeks apart (i.e., on September 1$^{st}$ and October 10$^{th}$) using identical synthesis conditions. The sols were tested on October 11$^{th}$, 2010. Thus the time from point of synthesis to Raman analysis was 1 day and 40 days. There was essentially no difference observed in the spectra (see Figure 26). This indicates that aging, at least for the MOE sol, appears to have no affect at all on the chemical makeup of the sol.

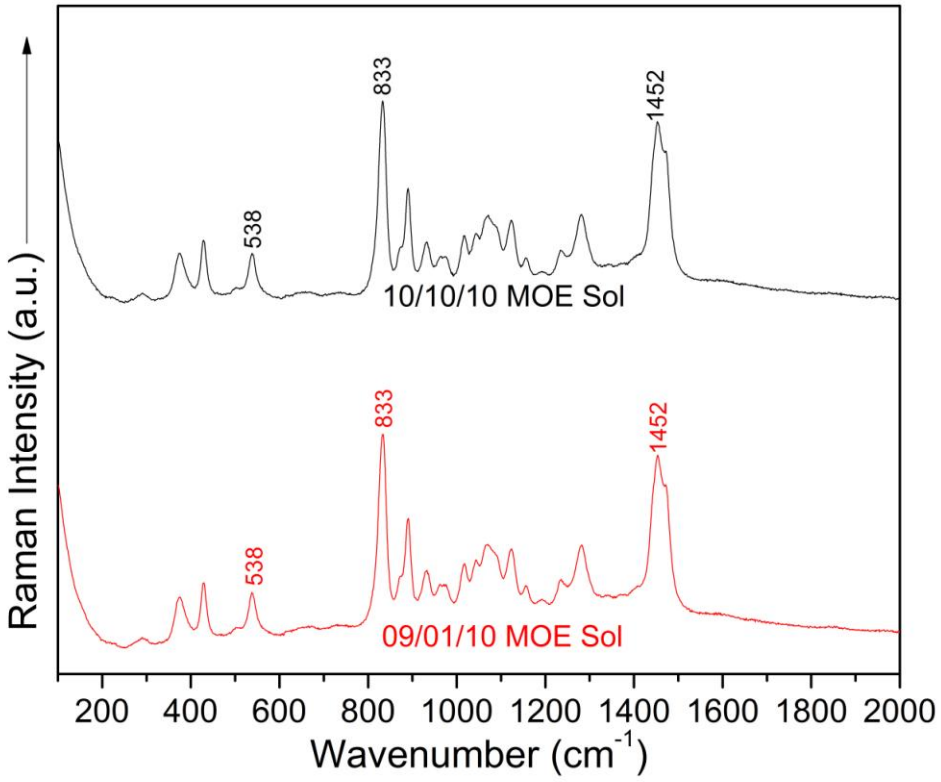


Figure 26: Raman Spectra of MOE Sol-Gel Fabricated Six Weeks Apart.

**Section III: Mechanistic Understanding of Sol Chemistry**

To assess the role that each precursor material has on the final sol chemistry, Raman spectra were taken of three sols (i.e., 0.5 M Zinc Acetate in MOE; n-Butanol and IPA) and compared to the Raman spectra of each precursor material used to make the sols.

- MOE Sol vs. Precursor Materials: The Raman MOE sol data is shown in Figure 27. The spectra have been offset to allow visual identification of all the key peaks. The Raman spectra were taken with acquisition time and cycles as follows: MOE Sol, 20 seconds, 5 cycles; MOE solvent, 10 seconds, 3 cycles; Zinc Acetate Dihydrate, 5 seconds, 2 cycles; Monoethanolamine 10 seconds, 3 cycles.

A close examination of the Raman spectra shows that the spectral pattern of the 'sol' is almost identical to spectral pattern of the solvent except for two peaks in the region of 930 $cm^{-1}$ and 970 $cm^{-1}$. Here the relative intensity of the MOE peaks shift. A close evaluation of the precursor Raman spectra indicate that the shift seen in the MOE sol relative to the MOE solvent cannot be attributed to precursor chemistry. Thus, there may be a unique chemistry taking place in the MOE sol. Whether this chemistry is a variable in the final film quality is outside of the scope of this paper but warrants further investigation.

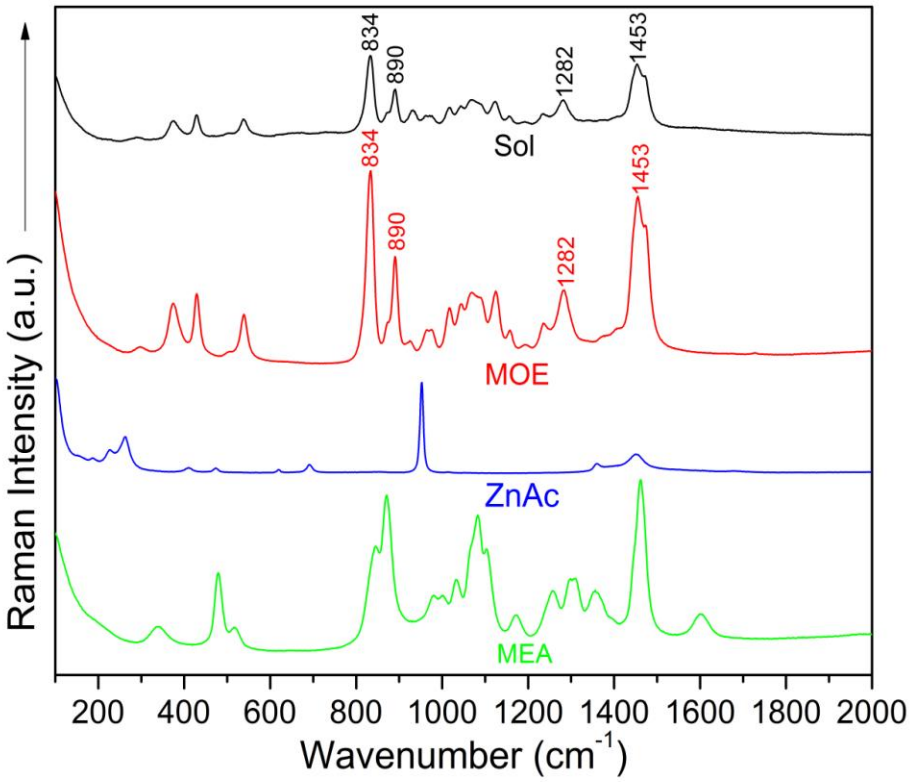


Figure 27: Raman Spectra of MOE sol and Precursor Materials.

- Butanol vs. Precursor Materials Chemistry: The Raman Butanol data is shown in Figure 28. The spectra have been offset to allow visual identification of all the key peaks. The Raman spectra were taken with acquisition time and cycles as follows: Butanol Sol, 20 seconds, 5 cycles; Butanol solvent, 10 seconds, 3 cycles; Zinc Acetate Dihydrate, 5 seconds, 2 cycles. A close examination of the Raman spectra shows that the spectral pattern of the 'sol' is almost identical to the spectral pattern of the solvent.

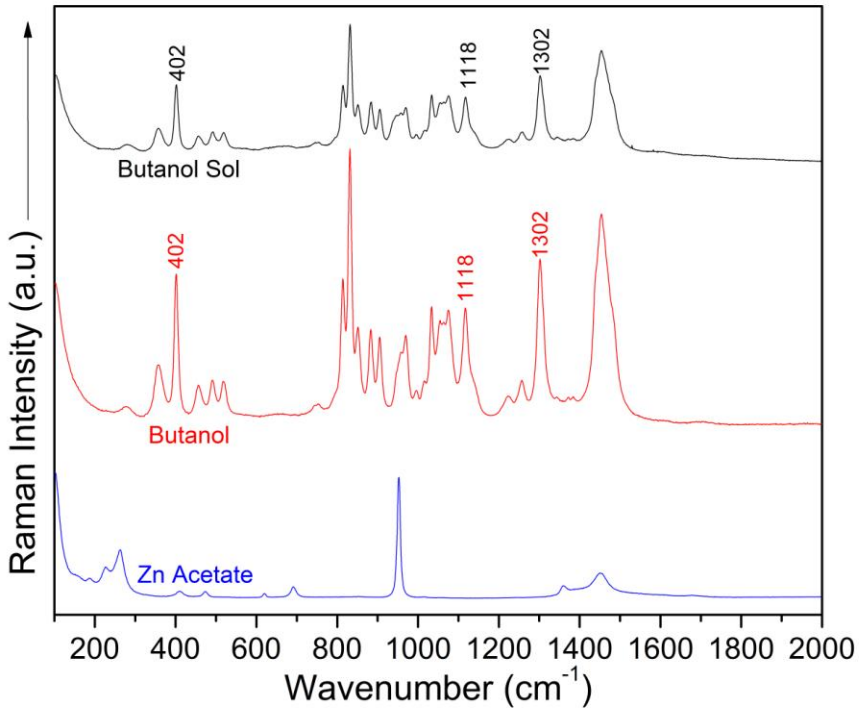


Figure 28: Raman Spectra of Butanol Sol and Precursor Materials.

- IPA vs. Precursor Materials Chemistry and 'self-assembly' ZnO film: The Raman IPA data is shown in Figure 29. The spectra have been offset to allow visual identification of the key peaks. The Raman spectra were taken with acquisition time and cycles as follows: IPA self-assembly film, 30 seconds, 3 cycles; IPA Sol, 5 seconds, 3 cycles; IPA solvent, 5 seconds, 3 cycles; Zinc Acetate Dihydrate, 5 seconds, 2 cycles. A close examination of the Raman spectra shows that the spectral pattern of the 'sol' is almost identical to the spectral pattern of the solvent. The spectral pattern of the film made from these precursor materials exhibited a peak showing at 996 $cm^{-1}$. Since this peak is not seen in the precursor materials or the sol, it is presumed to be an impurity that was introduced in the sol and/or film preparation. More will be said about the IPA 'self-assembly' film later in this report.

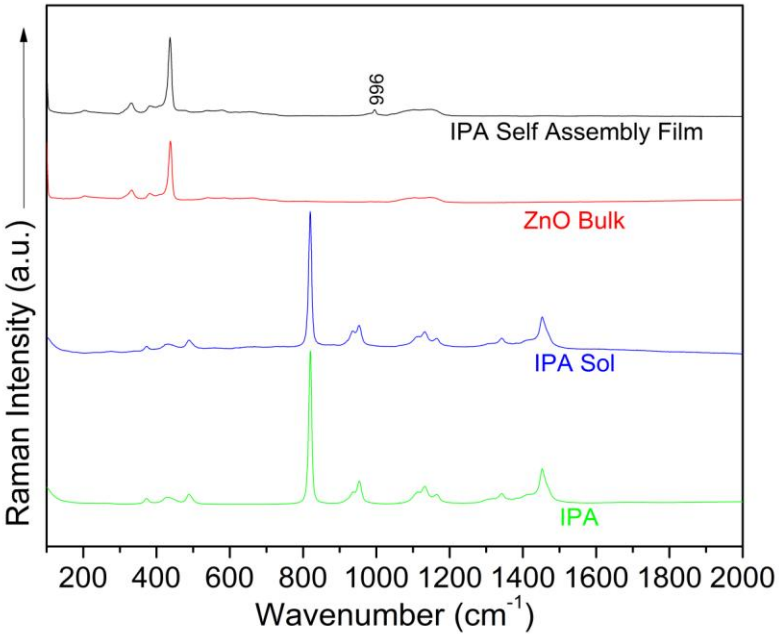


Figure 29: Raman spectra of IPA sol vs. Precursors & ZnO 'self-assembly' Film

- Methanol 'sol' to 'gel' Transition Chemistry: The Raman spectra of a 1.3 M Zinc Acetate in Methanol sol-gel was investigated to evaluate the solution transitions from 'sol' to 'gel'. Two hundred milliliters of a 1.3 M Zinc Acetate in Methanol sol was synthesized according to the process conditions described in Chapter 3. Part of this 'sol' was put in a tightly sealed vial. Then 60 grams of the 'sol' were placed directly into a 9 cm diameter Petri dish while the 'sol' was still hot. The Petri dish containing the 'sol' was left open to the air overnight. After 24 hours the 60 grams of 'sol' that had been placed in the Petri dish had reduced to 20 grams and had developed a distinct gel-like appearance. Specifically, the 'gel' was extremely viscous and sticky and had the faint visual evidence of a fine particulate in suspension. Also there was the faint beginning of a film depositing on a glass microscope slide that had been placed the Petri dish. In comparison, the 'sol' in the tightly sealed vial was water thin, colorless and homogeneous.

Raman spectra were collected for both the 'sol' and the 'gel' (Figure 30). The spectra have been offset to allow visual identification of the key peaks. The Raman spectra were taken with acquisition time and cycles as follows: Methanol Sol, 10 seconds, 3 cycles and the Methanol Gel, 20 seconds, 3 cycles.

The spectra show that the 'gel' has a number of distinctly different vibrational modes from the 'sol', many of which appear to be shifted and others are peaks that are not seen in any of the precursor materials nor are they ascribed to zinc oxide. This indicates that there are profoundly different interactions happening between the materials which make up the gel phase which cannot be traced to any of the individual precursor materials. Further research is needed to understand all the implications of these spectra changes.

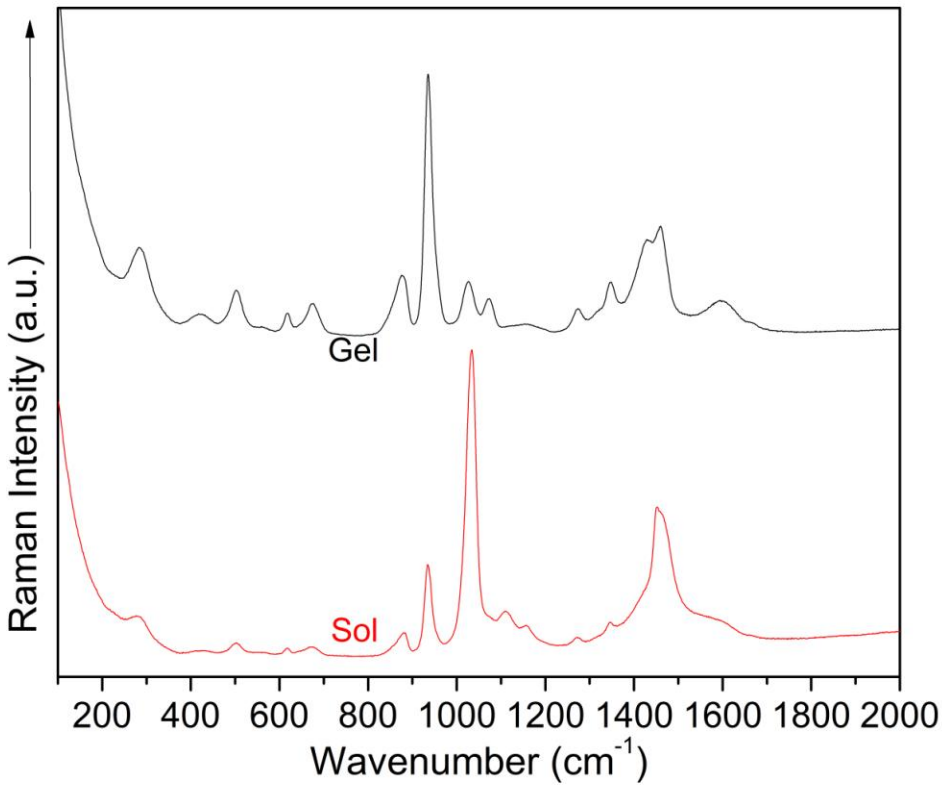


Figure 30: Methanol Sol-Gel Raman of Solution and Gel Phase

**Section IV: ZnO Films by Self- Assembly**

IPA 'Self-Assembly' ZnO Films: The development of the films with the 'self-assembly' approach is believed to be a slower form of the sol-gel mechanism. The solution of zinc-oxo-acetate clusters described earlier is allowed to gradually gel and form a solid skeletal structure of loosely connected nanoclusters at ambient conditions without thermal drying. Then, after a thick film is formed, an annealing step is done to condense the solid 'skeleton' into a good film.

This process can be done quickly with thermal drying or more slowly by allowing the substrate to remain in the sol for a day or two or a few weeks – depending on the solubility of the Zinc Acetate Dihydrate in the solvent as well as on the boiling point of the solvent.

The films made by thermal drying showed good optical transparency but were too thin for effective Raman spectroscopy investigations. The films made by 'self-assembly' are too thick to test for optical transparency but were sufficiently thick to produce a strong Raman signal. Therefore, Raman analyses of the 'self-assembly' films can provide insight to the ZnO sol-gel process (as discussed in the last section) and film quality.

A 'self-assembly' zinc oxide film was synthesized from a 0.5 M Zinc Acetate in IPA sol in a process similar to that described in Chapter 3. Specifically, a microscope slide (Pearl, precleaned, 1" by 3") that had been cleaned in boiling distilled water and then rinsed in acetone was taped to the side of a beaker in a vertical position and the IPA sol was placed in the beaker where it covered about two thirds of the microscope slide. After 30 days, a thick, white film had formed on the glass slides. The film was allowed to dry in air overnight then was thermally treated with an initial drying at $300^0$C for ten minutes followed by $500^0$C for 1 hour. The rate of heating the furnace was $5^0$ C/min. The films were allowed to cool in the furnace.

This was compared to a high purity, high quality Zinc Oxide bulk material ZnO films (Alfa Aesar, 99.99% purity). The Raman spectra settings for acquisition time and cycles were

as follows: IPA 'self-assembly' film and bulk, 30 seconds and 3 cycles. The spectra for the Zinc Oxide 'self-assembly' film and bulk samples are shown in Figure 31.

As mentioned earlier, Wurtzite Zinc Oxide has been reported (ref 42) to be characterized by a Raman peak at approximately 440 $cm^{-1}$. Thus, the peak at 438 $cm^{-1}$ in the spectra displayed in Figure 31 is the *E2* phonon and indicates that the desired Wurtzite crystal structure is present in the 'self-assembly' ZnO film. This is also confirmed by the comparison to the ZnO bulk material of high purity (99.99%) Wurtzite.

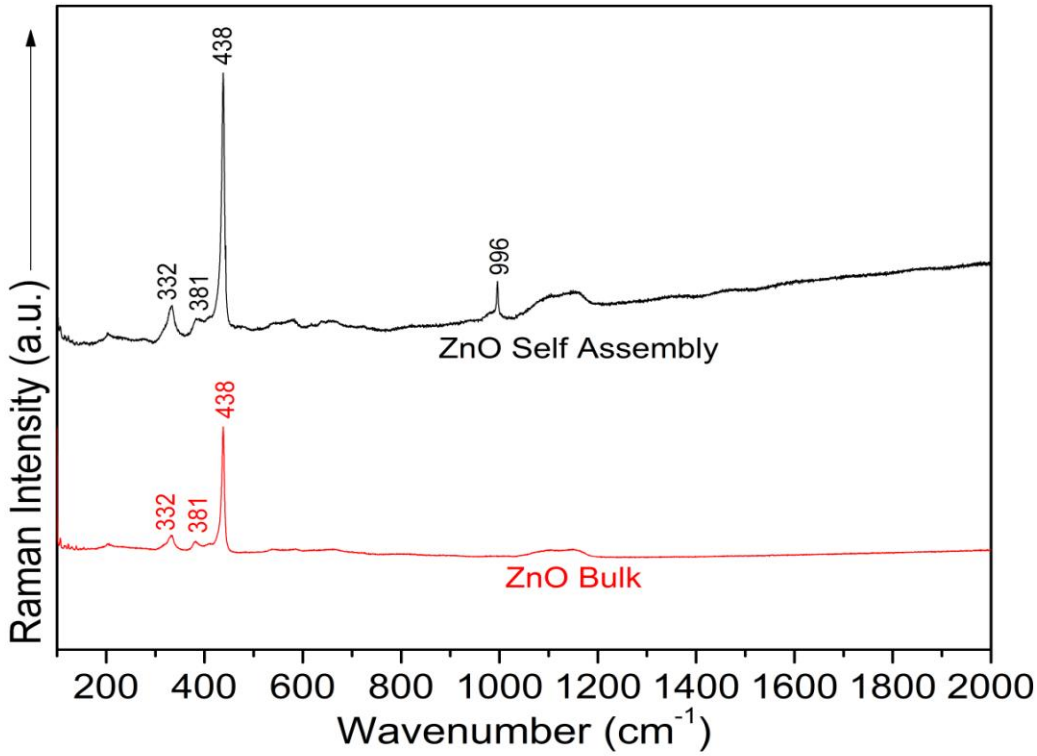


Figure 31: Raman Spectra of ZnO 'Self-Assembly' Film vs. ZnO Bulk

Note: The ZnO Self-Assembly fabricated by T.Y. Hill; the ZnO Bulk purchased from Alfa Aeser, 99.99% purity.

The peak at 584 $cm^{-1}$ has been ascribed in literature (ref 42 and many others) to the formation of defects such as absence of oxygen, interstitial zinc, and lack of free carriers. The fact that the 'self-assembly' ZnO film has little to no peak at this wavenumber means the crystal structure is relatively high quality with no defects.

The Raman band at 380 $cm^{-1}$ is ascribed to characteristic ZnO transversal modes. The peaks at 331 $cm^{-1}$ and 1150 $cm^{-1}$ are ascribed to ZnO second order modes. These are modes generally only appear if the ZnO film has a crystalline structure of high quality. The Raman spectra of the ZnO 'self-assembly' film shows the 331 $cm^{-1}$ peak and a slight 1150 $cm^{-1}$ peak. This provides further confirmation that the film is high-quality Wurtzite.

The sharpness of the *E2* phonon peak is an indication of the size of the microcrystalline grains forming in the sample. Sharper peaks indicate increased grain size. The ZnO 'self-assembly' films were found to have a full width at half height of 6.9 $cm^{-1}$ as compared to the ZnO bulk which was determined to be 6.4. $cm^{-1}$, indicating a larger grain size in the film.

As mentioned earlier, a shift in the film Wurtzite peak to a lower wavenumber relative to the bulk ZnO control would indicate that the film is under tensile stress and a shift to a higher wavenumber would indicate the film is under compressive stress (ref 42). There is no shift in the ZnO 'self-assembly' thin film Wurtzite band (438 $cm^{-1}$) relative to the bulk ZnO control (also at 438 $cm^{-1}$). This indicates that the 'self-assembly' thin film is not experiencing tensile or compressive stresses relative to the glass substrate. Also, the vibrational mode at 996 $cm^{-1}$ does not appear in the precursor materials and is therefore presumed to be an impurity that was introduced in the sol and/or in the film preparation.

Methanol 'Self-Assembly':

A 'self-assembly' Zinc Oxide thin film was made with a 1.3 M Zinc Acetate in Methanol sol. Specifically, the 'self-assembly' zinc oxide film was synthesized from a 1.3 M Zinc Acetate in Methanol sol using a process similar to that described in Chapter 3. Like the IPA 'self-assembly' film that was described earlier, this film was fabricated by taping a microscope slide (Pearl, precleaned, 1" by 3"; cleaned in boiling distilled water and then rinsed in acetone) to the side of a beaker in a vertical position and placing the Methanol sol in the beaker where it covered about two thirds of the microscope slide. In only 9 days (as compared with the 30 days necessary with the 0.5 M IPA sol), a thick, white film had formed on the glass slide. The film was allowed to dry in air overnight then was thermally treated at $500^0$C for 2 hours. The rate of heating the furnace was $5^0$ C/min. The film was allowed to cool in the furnace.

The Raman spectra are shown in Figure 32. The Raman spectra were recorded with an acquisition time of 10 seconds and averaged over 3 cycles. The resulting film shows the characteristic Wurtzite ZnO vibrational mode at 438 $cm^{-1}$. As mentioned earlier, the peak at 331 $cm^{-1}$ is ascribed to a ZnO second order mode. This mode is generally only evident if the crystalline structure is very good indicating that the Methanol 'self-assembly' film has good crystal structure. Finally, the 996 $cm^{-1}$ band seen in the Raman spectrum of the IPA 'self-assembly' does not appear in this spectrum. This may be simply that the impurity was not picked up in this process or it may be that the IPA process generates an impurity. It also could be a result of the longer and thus more effective annealing process (i.e., 1 hour vs. 2 hours). This will be a question for future research.

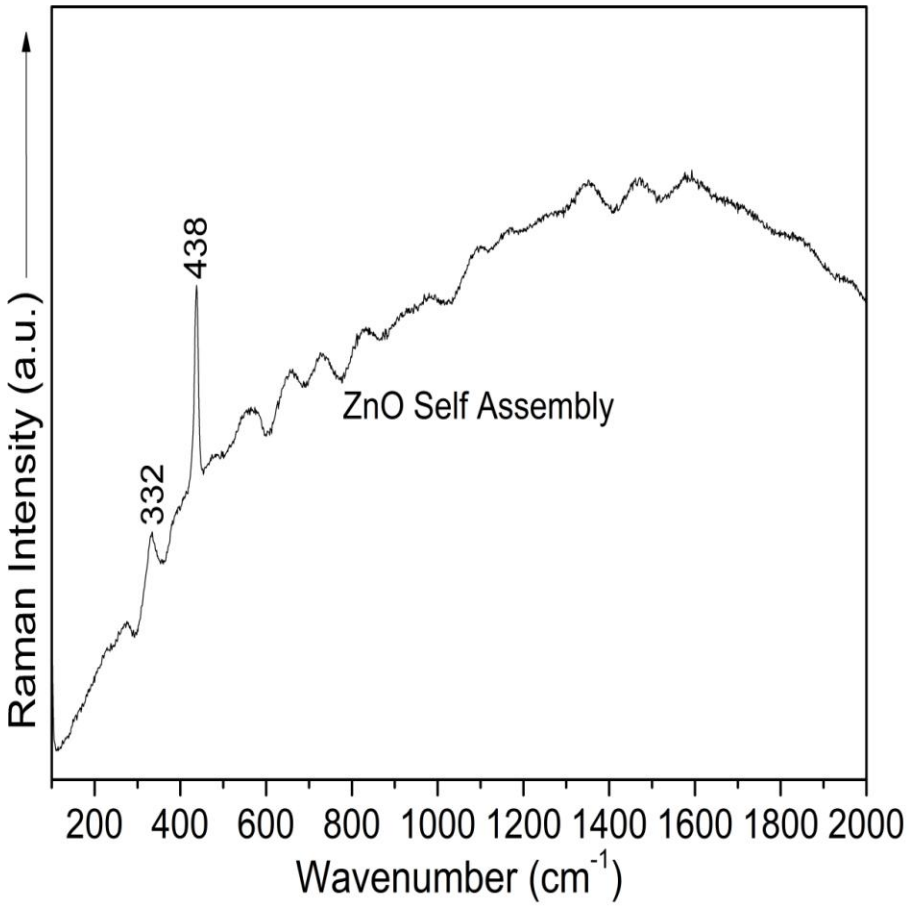


Figure 32: Zinc Oxide Thin Film formed by Methanol Sol-Gel 'Self-Assembly'

**Section V: ZnO Thin Films Thermal**

The Raman spectra of Zinc Oxide thin films that were developed with thermal treatments were extremely difficult to measure. The spectra, shown in Figure 33, reveal only a poor signal. Nevertheless, the characteristic Wurtzite ZnO vibrational mode at 438 $cm^{-1}$ is evident for the film annealed at $600^0$C confirming the desired Wurtzite crystal structure is in fact present.

The UV-Vis data discussed earlier indicated the presence of zinc oxide even at $150^0$C. Therefore, the absence of the characteristic Wurtzite vibrational mode in the Raman spectra of the ZnO films annealed at 150, 300, and $400^0$C is most probably due to the fact that the ZnO film is extremely thin and not enough material is present within the focal volume for a Raman investigation. More sensitive methods, such as surface-enhanced Raman spectroscopy, or the deposition of a thicker multi-layer ZnO film is suggested in this case.

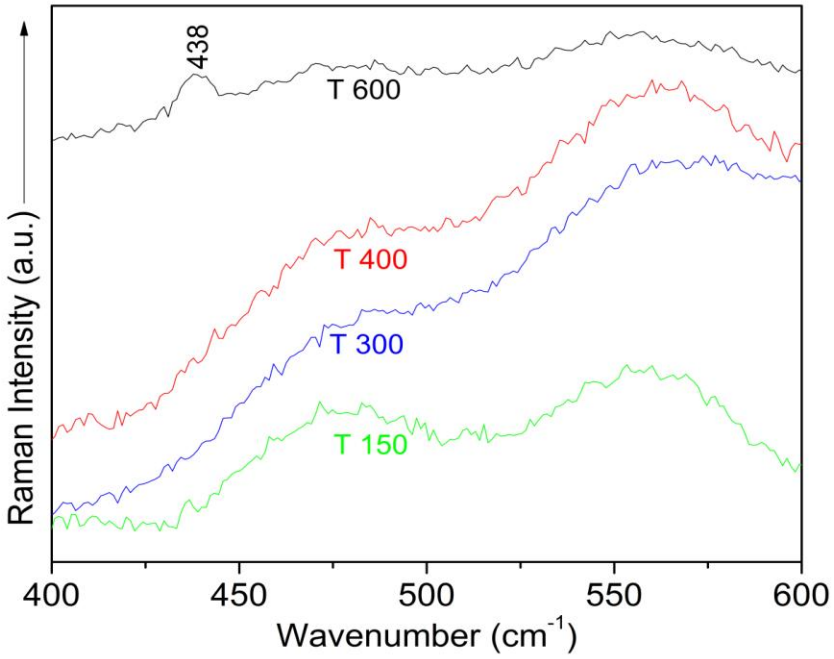


Figure 33 Raman Spectra of ZnO Thin Films with Thermal Annealing

To summarize, the use of Raman spectroscopy has shown:

- The sol-gel process is reproducible.
- The effect of aging is not a critical process variable.
- IPA and Methanol 'self-assembly' mechanism results in a high quality ZnO crystal structure.
- The chemistry of the MOE sol is slightly different from that of IPA and n-Butanol. This may be a factor in the slightly superior light transmission that was observed in the UV-Vis analyses.
- The Methanol 'sol' to 'gel' transition reveals startling vibrational mode shifts that should be explored further for mechanistic understanding.
- Raman spectra of ZnO thin films made via thermal treatment confirm the UV-Vis spectrophotometry results, that is, that the desired ZnO Wurtzite crystal structure has been formed.

# Chapter 7: Conclusions and Future Work

This report details the ways transparent conductive oxides (TCOs) are important to the emerging field of clean and renewable energy. It also discusses why Zinc Oxide is a particularly important TCO. Thus optimizing the fabrication of high-quality Zinc Oxide thin films at low cost was shown to play a significant role in the advancement of renewable energy technology commercialization. Because the sol-gel process is capable of mass producing high quality ceramic materials at low-cost, the overarching goal of this research was to assess the feasibility of using this process to fabricate of high quality Zinc Oxide thin films. In addition, key variables affecting Zinc Oxide sol-gel processing were evaluated and the resulting films characterized for important TCO parameters such as optical transparency and crystal structure. Chemical reaction mechanisms within the sol-gel process were also studied to advance the fundamental understanding of Zinc Oxide thin film fabrication via sol-gel. The resulting research findings revealed a number of important insights as well as several directions for future work as follows:

- A one step sol-gel Zinc Oxide process is a feasible way to fabricate high quality Zinc Oxide films with optical transparency of 90% as well as high quality Wurtzite crystal structure. Specifically, a 0.5 M Zinc Acetate organic based sol-gel process was developed that was capable of fabricating high quality thin films by placing a droplet of sol on a microscope slide followed by 'in air' thermal treatment. This process could be easily scaled to commercial levels using techniques such as ink jet printing or spray coating the 'sol' onto the substrate prior to thermal treatment. Future work should be to scale up the fabrication process using applications methods such as these to produce larger films. This research also indicated that a one-step thermal treatment was acceptable. Future work should confirm this since it would further reduce the complexity of manufacturing energy intensiveness. As part of the thermal treatment investigation, it will be essential to determine the time and the temperature that is needed to remove all the precursor impurities. In addition, exact characterization of the film thickness, with elipsometry, and crystallinity, via x-ray diffraction, is needed.

- The chemical and physical properties of the solvent are extremely important to the final Zinc Oxide film quality. The most optically transparent films using organic solvents were those made with MOE as the solvent and thermally annealed in one step to a temperature of at least $400^0$C. This appears to be partly due to the relatively high boiling point of MOE compared to other organic solvents. MOE's boiling point is in the temperature range that coincides with the initial condensation of Zinc Oxide nanoparticles. Raman spectroscopy also reveals a subtle sol-gel chemistry that is unique to MOE vs. other organic solvents (i.e., that are based on hydrocarbons with an alcohol functional group such as IPA and n-Butanol). It is not known at this point to what extent the unique MOE chemistry plays to the final film quality vs. its physical properties, i.e., boiling point. Future research should explore the quality of films as a function of solvent boiling point; sol-gel chemistry and annealing/drying process. These variables are interconnected and understanding the exact mechanisms will lead to optimization of an organic-based sol-gel process.
- The sol-gel process developed in this research is extremely reproducible. Well controlled mixing of the precursor ingredients for two hours at a temperature just below the solvent boiling point provided extremely consistent results in the resulting sol-gel mixture and the subsequent ZnO film that were formed. There was essentially no difference observed in the Raman spectra of two 0.5 M MOE 'sols' that were made more than a month apart but tested via Raman spectroscopy at the same time. Highly transparent films were also reproducible from the MOE sol-gel process. In addition, MOE based sol-gel is more stable than the sol-gel based on alcoholic hydrocarbons. 'Aging' of the 'sol' is not a critical process variable as has been suggested in literature. This indicates that aging, at least for the MOE sol, appears to have no affect at all on the chemical makeup of the sol. This 'aging' insight is an important departure from what has been reported in literature.
- A unique 'self-assembly' sol-gel method has been discovered that yields high quality Zinc Oxide films without thermal drying. IPA and methanol have both been shown to be solvents that will spontaneously form Zinc Oxide films at concentrations of 0.5 M and 1.3M Zinc Acetate. Raman analyses of films made by 'self-assembly' from a 0.5 M Zinc Acetate in IPA sol and from a 1.3 M Zinc Acetate in Methanol sol show the characteristic Wurtzite

vibrational modes and second order modes indicative of high quality crystal structure. Further work needs to be done to explore and optimize the 'self-assembly' process as well as the final film properties that are obtained from this fabrication approach. As part of this future research, investigation into whether the 'sol' can it be recycled is warranted because the majority of solvent is not consumed in thermal treatment. Recycling the organics would greatly enhance the cost effectiveness as well as environmental friendliness of an organic based sol-gel approach.

- The feasibility of using water as the solvent for ZnO sol-gel needs additional research but shows promise. A clear and stable water based sol produced using 0.5 M Zinc Acetate Dihydrate with 0.5 M Citric Acid and a small amount of Ammonium Hydroxide to provide a pH of 6 to 8 was identified. Like the organic based sol-gels, the pH must still be alkaline to make the hydroxyl groups available. However, to stabilize the 'sol', the addition of citric acid is required, which probably acts as a chelating agent. Although this is a stable sol, it will not form films on glass slides. It could have potential applications for forming nanostructures with templates and/or forming films on more hydrophilic substrates. Using the water sol in template applications could be an excellent way to make various devices such as the electrode base for the DSSC. This would be a very interesting area for future work.
- A range of polymeric thickeners were evaluated as stabilizing agents for the water sol-gel. These included Polyvinyl Alcohol, Hydroxyethyl Cellulose, Xanthan Gum, and Guar Gum as film forming 'sol-gel' additives. The best films were those made with a sol that contained only water, Zinc Acetate Dihydrate, and a nonionic film forming additives. With this modification good films were developed that were **crystal** clear and in fact looked quite different – visually – from the films made with organic solvents. However, the films were not homogeneous in thickness and there was still evidence that the sol was beading up on the glass substrate to some extent. It was clear that substantial formulation work would be needed to use water as a solvent that would yield consistent film results. Nevertheless, water based sols hold the promise of tremendous cost effectiveness as a sol-gel process. In addition the films appeared to form unique ZnO film morphology. Continue formulation work on water based ZnO sol-gel to get a rheology that facilitates homogenous film formation is warranted.

The thermal treatment of these films needs to be studied to evaluate optimal conditions for condensing the 'sol' to the final ceramic material. Raman spectroscopy should be done to better understand the chemical mechanisms involved in the water based sol-gel and to characterize the thin films.

- While an alkaline pH has been confirmed as essential to Zinc Oxide thin film sol-gel chemistry, the specific pH modifier MEA does not appear to be essential and can be interchanged with other similar pH modifiers such as ammonium hydroxide. The Acetate group, on the other hand, that is introduced through the use of Zinc Acetate is believed to be a key stabilizing agent in the chemistry that leads to films. A model for how the Acetate ion aids film formation is proposed that can be likened to that which occurs in surfactant chemistry. This builds on models presented in literature (Ref 5,6, 9 and 30) as described in Chapter 2 and depicted in Figure 8: Zinc Acetate Sol-Gel Chemistry.

In the surfactant chemistry, a micelle is formed at the critical micelle concentration of surfactant in water. At these relatively low surfactant concentrations, the surfactant forms a spherical phase consisting of the hydrophilic end of the surfactant towards the water solvent and the hydrophobic end towards the center of the spherical micelle (see Figure 34). At increased surfactant concentrations in water, the surfactant transitions first to a liposome structure which is a tube like structure. Then at higher surfactant concentrations a 'bilayer sheet' structure emerges. In the 'bilayer sheet' the water phase is sandwiched between layers of surfactant with the hydrophilic end of the surfactant forming loose bonds with the water phase and the hydrophobic ends of the surfactant pointing towards a central surfactant lamellar sheet. In this way stacks of bilayers sheets can be formed and these sheets, having limited mobility, can be very highly viscous.

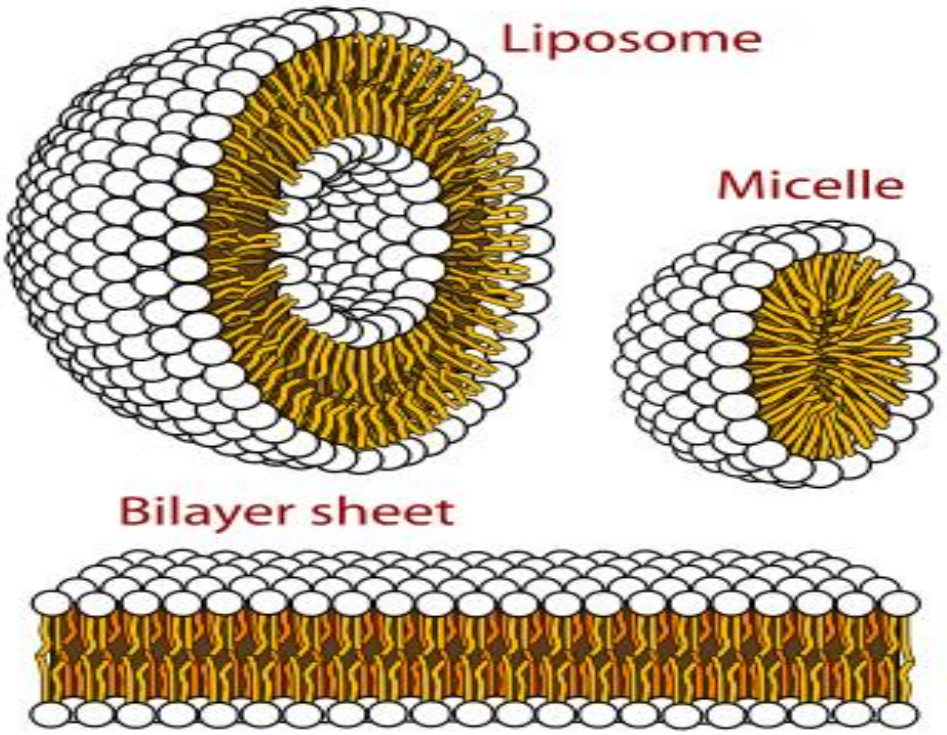

Figure 34: Surfactant Phases (ref 77)

An analogous model could describe the Zinc Acetate sol-gel chemistry. Specifically, the alkaline pH allows the formation of $Zn(OH)_2$ which through condensation shown in Equation 6 can form ZnO. However, if this reaction were to occur directly from Zinc Acetate to Zinc Hydroxide to Zinc Oxide, there would likely be immediate precipitation from the solvent to form a particulate of Zinc Oxide rather than a film. This is based on the fact that $Zn(OH)_2$ and ZnO are very insoluble in water and hydrocarbons. Yet Zinc Oxide clearly does not precipitate as the 'sol' transitions to the 'gel' phase. A fine particulate however, that is suspended in the 'gel' is observed and the viscosity greatly increases when the gel becomes highly concentrated.

An intermediary moiety is likely formed in the sol-gel process that facilitates the transition from integrated, cross linked nanoparticles to the final films of Zinc Oxide thin film. The chemistry of this intermediary is likely to be some type of Zinc Hydroxy Acetate combination. As condensation to nanoparticles occurs, structures with a hydrophilic center would be

increasingly made up mostly of ZnO with a hydrophobic surface made up of hydroxyl and acetate groups, as shown in Figure 35. The center of the nanoparticle would consist of ZnO but the surface would have a zinc ion (+2) that is attached to one hydroxyl group leaving a strongly positive charged surface that the acetate groups would complex with. The organic solvents, having both a hydrophilic end, composed mostly the hydroxyl group of the alcohol functional group, and a hydrophobic end which is the hydrocarbon end, would fill in the gaps between nanoclusters. This would stabilize the nanoclusters and simultaneously provide the means for the growth of larger more oriented ZnO that ultimately connects into lamellar sheets similar to the surfactant chemistry discussed earlier.

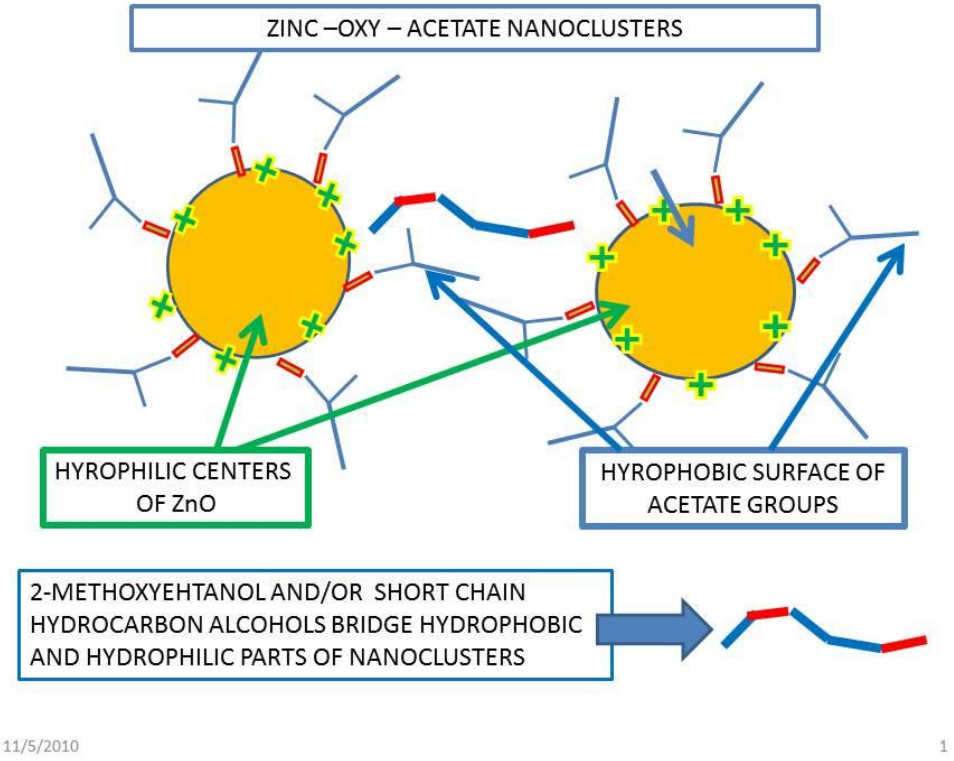


Figure 35: Proposed Model for Organic Solvent Bridging Mechanism

This model might explain why the 2-methoxyethanol sols show uniquely robust stability relative a hydrocarbon with similar molecular weight and/or boiling point but with one hydrophilic functional group at each end i.e. a hydroxyl group and a ketone group. It is

possible that the ketone group that exists on MOE also helps to 'emulsify' and bridge the nanoparticles or micelle like groups of Zinc –Hydroxy –Acetate.

This model also helps to explain the more challenging formulation of a water based Zinc Acetate sol-gel. Water would be incompatible with the 'Acetate' and would thus result in the immediate formation of Zinc Oxide, as was in fact the case. The polymers that stabilized the water solvents were generally nonionic and had lots of hydroxyl functional groups to provide hydrogen bonding with the zinc-hydroxy entity. It's possible that the Acetate group is unnecessary in water based sol-gels with polymers present. In addition, it's expected that the polymer provides the suspension system for the transition from particulate to film rather than an extensive metal – hydroxide particle to particle cross linking. Net, a very different mechanism for forming the final Zinc Oxide film is likely happening. This is a fascinating possibly with much potential for exploration in future work.

Table 13: Material Properties

| Material | Molecular Formula | Chemical structure | Molecular weight (g/mol) | Boiling Point ($^0$C) | Density ( g/cm$^3$) | Surface Tension (mN/m) |
|---|---|---|---|---|---|---|
| 2 Methoxyethanol | $C_3H_7O_2$ | 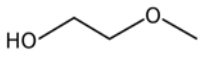 | 76 | 125 | 0.97 | 32 |
| n-Butanol | $C_4H_9$ OH | 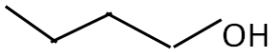 | 74 | 118 | 0.81 | 24 |
| Isopropanol | $C_3H_7OH$ | | 60 | 82 | 0.79 | 22 |
| Ethanol | $C_2H_5OH$ | | 45 | 78 | 0.79 | 22 |
| Methanol | $CH_3OH$ | C – O H | 32 | 65 | 0.79 | 23 |
| Water | H $_2$ O | H – O – H | 18 | 100 | 1 | 70 |
| Monoethanolamine | $C_2H_7NO$ | | 61 | 170 | 1 | NA |
| Citric Acid | $C_6H_8O_7$ | 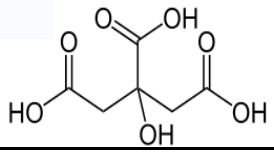 | 210.14 | Decomposes at 175 °C | NA | NA |

## Bibliography


1. O'Brien, Shane, Koh, L.H.K, Crean, Gabrien M., ZnO thin films prepared by a single step sol-gel process, Thin Solid Films, 516, 2008.
2. Srinivasan, G., Kumar, J., 'Optical and structural characterization of Zinc Oxide thin films prepared by sol-gel process' Crystal Research Technology, 41, No. 9, 893 (2006).
3. Hongxia Li, Jiyan Wang, Hong Liu, Huaijin Zhang, Xia Li, 'Zinc Oxide films prepared by sol-gel method', Journal of Crystal Growth 275 (2005) e943-e946.
4. Natsume, Y., Sakata, H, 'Zinc oxide films prepared by sol-gel spin-coating',Thin Solid Films 372 (2000) 30-36.
5. Kamalasanan, M. N., Chandra, Subhas, 'Sol-gel synthesis of ZnO thin films', Thin Solid Films 288 (1996) 112 -115.
6. Jin-Hon Lee, Kyung-Hee Ko, Byung-Ok Park. 'Electrical and optical properties of ZnO transparent conducting films by the sol-gel method', Journal of Crystal Growth, 247 (2003) 119-125.
7. Raoufi, Davood, Raoufi, Taha. 'The effect of heat treatment on the physical properties of sol-gel derived ZnO thin films', Applied Surface Science, 255 (2009) 5812-5817.
8. Kamalasanan, M. N., Chandra, Subhas. 'Sol-gel synthesis of ZnO thin films'. Thin Solid Films. (1996) 112-115.
9. Znaidi, L, Soler Illia, G. J. A. A et al. 'Oriented ZnO thin films synthesis by sol-gel process for laser application'. Thin Solid Films. (2003) 257-262.
10. Znaidi, L, Soler Illia, G. J. A. A, Kanaev, A. 'Elaboration of ZnO Thin Films with Preferential Orientation by a Soft Chemistry Route'. Journal of Sol-Gel Science and Technology. 2003.
11. Bao, Dinghua, Gu, Haoshuang, Gu, Kuang, Anxiang. Sol-Gel derived c-axis orented Zno thin films'. Thin Solid Films. 1998.
12. Choi, Byeong Kyun, Chang, Dong Hoon et al, 'Optical characterization of ZnO thin films deposited by Sol-gel method'. Journal of Material Science. 2006.

13. Zhang, Canyun. High-quality oriented ZnO films grown by sol-gel process assisted with ZnO seed layer'. Journal of Physics and Chemistry of Solids. 2010.
14. Petersen, J., Brimont, C. et all, Optical properties of ZnO thin films prepared by sol-gel process". Microelectronics Journal. 2009.
15. Ohyama, Masashi, Kozuka, Hiromitsu, Yok, Toshinobu. 'Sol-Gel Preparation of Transparent and Conductive aluminum-Doped zinc Oxide Films with Highly Preferential Crystal Orientation'. Journal of the American Ceramic Society. 1998.
16. Copuroglu, Mehmet, Koh, Lee Huat Kelly et al. 'Comparative characterization of zinc oxide thin films prepared form zinc acetate with or without water of hydration via the sol gel method'. Journal of Sol-Gel Technology. 2009.
17. Delgado, G. Torres, Romero, C. I. Zuniga et al. 'Optical and structural properties of the sol-gel-prepared ZnO thin films and their effect on the photcatalytic activity'. Solar Energy Materials & Solar Cells. 2009.
18. Lin, Li-Yu, Kim, Dae-Eun. 'Effect of annealing temperature on the tribological behavior of ZnO films prepared by sol-gel method'. Thin Solid Films. 2009.
19. Kingery, W.D., Introduction to Ceramics. Wiley Publishing. 1960, 1076.
20. Goetzberger, A., Hoffmann, V.U. Photovoltaic Solar Energy Generation. New York. Springer. 2005.
21. Zhang, Yang, Lin, Bixia et al. 'Strong Ultraviolet emission and Rectifying Behavior of nanocrystalline ZnO films'. Optical Materials. 2006.
22. Zhang, Y. L., Yang, Y. et al. Preparation of ZnO Nanoparticles by a Surfactant-assisted complex sol-gel method using Zinc Nitrate'. Journal of Sol-Gel Technology. 2009.
23. Zhan, Rong, Kerr, Lei L. 'A Simple Method for Systematically Controlling ZnO Crystal Size and Growth Orientation'. Solid State Chemistry. 2007.
24. Yue, H. Y., Fei, W. D. 'Sol-gel process of ZnO and ZnAl2O4 coated aluminum borate whiskers'. Journal of sol-Gel Technology. 2007.
25. Modelaers, D, Vanhoyland, G. et al. 'Chemical Solution Deposition of ZnO Thin Films by an Aqueous Solution Gel Precurser Route'. Journal of Sol-Gel Science and Technology. 2003.

26. Von Roedern, B., Ullal, H.S. 'The role of Polycrystalline Thin-Film PV Technologies in Competitive PV Module Markets' National Renewable Laboratories. San Diego. May 2008 NREL/CP-520-42494.
27. Falah S. Hasoon, Hamda A. Al-Thani*, Xiaonan Li, Ana Kanevce, Craig Perkins, and Sally Asher. 'Investigation of the Effect of I-ZnO Window Layer on the Device Performance of the Cd-Free CIGS Based Solar Cells'. National Research Energy Laboratory. 2008.
28. Soga, Tetsuo. Nanostructured materials for Solar Energy Conversion. Elsevier. Amsterdam, Netherlands. 2006.
30. 'Solar Cells Overview'. SPECMAT. http://www.specmat.com/solar%20cell%20specmat.html. 2010.
31. Spanhel, Lubomer. 'Colloidal ZnO nanostructures and functional coatings: A survey'. Journal of Sol-Gel Technology. 2006.
32. Spanhel, Lubomer, Anderson, Marc A. 'Semiconductor Clusters in the Sol-Gel Process: Quantized Aggregation, Gelation, and Crystal Growth in Concentrated ZnO Colloids'. Journal of the American Chemistry Society. 1991.
33. Grasset, Fabien, Starukh, Galina et al. 'From ZnO Colloids to Nanocrystalline Colored ZnxTiyOw-zNz Spinel Films'. Advanced Materials. 2005.
34. Bonanni, M., Shanhel, L, et al. 'Conversion of Colloidal ZnO-WO3 Heteroaggregates into Strongly Blue Luminescing ZnWO4 Xerogels and Films'. Chemical Materials. 1998.
35. Van Werde, K., Modelaers, D., et al. 'Thermal Decomposition of the ammonium zinc acetate citrate precursor for aqueous chemical solution deposition of ZnO'. Journal of Materials Science. 2002.
36. Choi, Kyoung-Shin, Steinmiller, Ellen M.P. 'Electrochemical Synthesis of lamellar structured ZnO films via electrochemical interfacial surfactant templating'. Electrochimica Acta. 2008.
37. Wang, Jinzhong, Du, Guotong, et al. 'Luminescence properties of ZnO films annealed in growth ambient and oxygen'. Journal of Crystal Growth. 2004.

38. Zinc oxide crystal structure images. http://en.wikipedia.org/wiki/Zinc_oxide. 9/9/10. Cheyney, Tom. 'Sunny for Small Tech in Solar' Small Times. PennWell.
39. 'Antireflective coatings'. http://pvcdrom.pveducation.org/index.html. PVCDROM Honsberg & Bowden. September 2010.
40. Jimenez-Sandoval, S. 'Micro-Raman spectroscopy: a powerful technique for materials research'. Microelectronics Journal. 2000.
41. Lakshmi, Brinda B, Dorhout, Peter K., Martin, Charles R., 'Sol-Gel Template Synthesis of Semiconductor Nanostructures'. Chem Mater. 1997.
42. Yahia, S. Ben. 'Raman study of oriented ZnO thin films deposited by sol–gel method'. Spectrochimica Acta Part A 71 (2008).
43. Kudelski, Andrzej. 'Analytical applications of Raman spectroscopy'. Talanta. 2008.
44. Francisco, P. S. C. et al. 'Structures and Vibrational Spectra of CH3OCH2CH2OH: The Hydrogen-bonded Conformers'. J. Chem. Soc. Faraday Trans. 1994.
45. Goldenblum, A et al. 'Optical properties of ZnO nanocrystallites embedded in a gold-oxide matrix'. Journal of Optoelectronics and Advanced Materials. 2006.
46. Shan, Guiye et al. 'Enhanced Rman Scattering of ZnO Quantum Dots on Silver Colloids'. J. Phys. Chem. 2007.
47. Dong, Z. W. et al. 'Raman Spectra of single micrometer-sized tubular ZnO'. Materials Chemistry and Physics. 2009.
48. Vernardou, D. et al. 'pH effect on the morphology of ZnO nanosturctures grown with aqueous chemical growth'. Thin Solid Films. 2007.
49. Castanedo-Perez, R. et al. 'Influence of annealing temperature on the formation and characteristics of sol-gel prepared ZnO films'. J. Vac Sci. Technol. 1999.
50. Amorim da Costa, A. M. et al. 'Molecular aggregation in neat 2-Methoxyethanol and in 2-Methoxyethanol/acrylamide solutions – A study by Raman spectroscopy and ab initio calculations' Vibrational Spectroscopy. 2006.
50. Brioude, A. et al. 'Raman spectroscopy of sol-gel ultrathin films enhanced by surface plasmon polaritons' Journal of Applied Physics. 2000.

51. Li, Zhi-Yang, Xu, Fuchun et al. 'Zinc oxide thin film synthesized by combustion chemical vapor deposition'. Applied Surface Science. 2008.
52. Kappertz, O. et al. 'Reactive sputter deposition of zinc oxide: Employing resputtering effects to tailor film properties'. Thin Solid Films. 2005.
53. Heo, Y. W. et al. 'Origin of green luminescence in ZnO thin film grown by molecular-beam epitaxy'. Journal of Applied Pyhsics. 2005.
54. Sbrockey, Nick, Ganesan, Shanthi. 'ZnO thin films by MOCVD'. www.three-fives.
55. Villanueva, Yolanda et al. 'Pulsed laser deposition of zinc oxide'. Thin Solid Films. 2006.
56. Krunks, Malle, Mellikov, Enn. 'Zinc oxide thin films by the spray pyrolysis method'. Thin Solid Films. 1995.
57. Mosbah, A. et al. 'Comparison of the structural and optical properties of zinc oxide thin films deposited by d.c. and r.f. sputtering and spray pyrolysis'. Surface Coatings & Technology. 2005.
58. Green Econometrics. 'Understanding the Cost of Solar Energy' 05/04/09. http://greenecon.net/understanding-the-cost-of-solar-energy/energy_economics.html.
59. Martins, R et al. 'Zinc Oxide as an ozone sensor'. American Institute of Physics. 2004.
60. Wang, J. X. et al. ' Zinc oxide nanocomb biosensor for glucose detection'. Applied Physics Letters. 2006.
61. Fuhs, Walther. 'Chapter 17 ZnO Window Layers for Solar Cells'. Springer. 2005.
62. Chopra, K. L., 'Thin-Film solar Cells: An Overview'. Progress in Photovoltaic's: Research and Applications. 2004.
63. Willander, M. et al. 'Fundamentals and properties of zinc oxide nanostructures: Optical and sensing applications'. Superlattices and Microstructures. 2008.
64. Ozgur, U. et al. 'A comprehensive review of ZnO materials and devices'. Applied Physics Review. 2005.
65. Lin, Yuan-Hua et al. 'Room-temperature ferromagnetic and ferroelectric behavior in polycrystalline ZnO-based thin films'. Applied Physics Letters. 2007.
66. Pearton, S.J. 'Recent progress in the processing and properties of ZnO'. Progress in Materials Science . 2005.

67. Sahay, P. P. 'Zinc oxide thin film gas sensor for detection of acetone'. Journal of Materials Science. 2005.
68. Suchea, M. et al. 'ZnO transparent thin films for gas sensor applications'. Thin Solid Films. 2006.
69. Mitra, P. et al. 'ZnO thin film sensor'. Materials Letters. 1998.
70. Singh. S. P. et al. 'Cholesterol biosensor based on rf sputtered zinc oxide nanoporous thin film'. Applied Physics Letters. 2007.
71. Sayhan, Ilker et al. 'Dye and polymer based light sensor for tag integration'. Microsyst Technol. 2008.
72. Lowe, Mark et al. 'Thin-film force sensors: opening doors in automated systems'. Sensor Review. 2007.
73. 'Ultraviolet-Visible (UV-Vis) Spectroscopy Background Information'. http://www.ucmo.edu/chemphys/about/documents/cary_300_bio_uv.pdf. September 7, 2010.
74. 'Visible and Ultraviolet Spectroscopy'. 'http://www2.chemistry.msu.edu/faculty/reusch/VirtTxtJml/Spectrpy/UV-Vis/spectrum.ht. September 7, 2010.
75. Kyaw, A. K. K. et al. 'Efficient charge collection with sol–gel derived colloidal ZnO thinfilm in photovoltaic devices'. J Sol-Gel Sci Technol (2009).
76. Callister, William D. Materials Science and engineering an Introduction. John Wiley and Sons. 2007.
77. Micelle. http: //en.Wikipedia.org/wiki/Micelle. November 6, 2010.